Insights into anterograde trafficking and pharmacological chaperoning of Cannabinoid Receptor 2 (CB_2)

Caitlin RM Oyagawa [1,2], Braden Woodhouse [1,2,3], Karren C Wood [1,2], Michelle Glass [1,2,4,5], Natasha L Grimsey * [1,2,5]

[1] Department of Pharmacology and Clinical Pharmacology, School of Medical Sciences, Faculty of Medical and Health Sciences, University of Auckland, Auckland, New Zealand

[2] Centre for Brain Research, Faculty of Medical and Health Sciences, University of Auckland, Auckland, New Zealand

[3] Department of Oncology, School of Medical Sciences, Faculty of Medical and Health Sciences, University of Auckland, Auckland, New Zealand

[4] Department of Pharmacology and Toxicology, School of Biomedical Sciences, University of Otago, Dunedin, New Zealand

[5] Maurice Wilkins Centre for Molecular Biodiscovery, New Zealand

* Correspondence: n.grimsey@auckland.ac.nz (N L Grimsey)

Author ORCiDs:

CO – https://orcid.org/0000-0001-9533-4801

BW – https://orcid.org/0000-0001-7162-6199

KW – https://orcid.org/0000-0002-9932-2936

MG – https://orcid.org/0000-0002-5997-6898

NG – https://orcid.org/0000-0003-3941-4537

Author contributions: Conceptualisation: NG, MG, CO; Investigation: CO, BW, NG, KW; Methodology: NG, CO; Visualization: CO, KW, NG; Supervision: NG, MG; Funding acquisition: NG; Project administration: NG; Writing – original draft: CO, NG; Writing – review & editing: All authors.

Acknowledgements: This research was funded by a Marsden Fast-Start grant from the Royal Society Te Apārangi New Zealand (UOA1507). CO was supported by a University of Auckland Doctoral Scholarship. NG was supported by Fellowships from the Auckland Medical Research Foundation (1313001) and the Health Research Council of New Zealand (20-006).

Abstract

Cannabinoid Receptor 2 (CB_2) is a promising therapeutic target for modulating inflammation. Canonical signalling responses to receptor ligands are critically dependent on cell surface receptor expression. However, it is also now appreciated that intracellular G protein-coupled receptors can contribute to signalling responses and influence functional outcomes. Therefore, understanding how the subcellular distribution of receptors is controlled is also highly pertinent. CB_2 is observed to be expressed at the cell surface as well as having a considerable proportion expressed intracellularly. Despite this distribution being well established, little is known about the regulation of CB_2 anterograde trafficking and subcellular distribution. We report that sustained stimulation with a range of CB_2 agonists concurrently internalises cell surface human CB_2 and stimulates a distinct population of CB_2 to be delivered to the cell surface, at various expression levels. We present evidence that the ligand-stimulated anterograde trafficking is a result of CB_2 agonists, as well as inverse agonists, acting as pharmacological chaperones. We also report that a di-lysine (KK) motif in the CB_2 C-terminal tail is required for basal delivery to the cell surface. Corroborating the hypothesis that CB_2 ligands can act as pharmacological chaperones, sustained CB_2 ligand stimulation induces cell surface expression of the mutated receptor and alters maturation states as measured by western blotting. Our finding that CB_2 ligands can unconventionally manipulate CB_2 cell surface expression may well have important implications for optimal design of CB_2-targeted therapeutics.

Keywords: Receptor, Cannabinoid, CB2; Cannabinoid Receptor Modulators; Receptors, G-Protein-Coupled; Intracellular Trafficking; Pharmacological Chaperone; Molecular Mechanisms of Pharmacological Action; Amino Acid Motifs; Intracellular Membranes; Signal Transduction; Inflammation.

1 Introduction

Cannabinoid Receptor 2 (CB_2) is a class A G protein-coupled receptor (GPCR) that is predominantly expressed in immune tissues and cells, with functions including modulation of immune cell migration, chemotaxis, differentiation, and synthesis of cytokines, with predominantly immunosuppressive and anti-inflammatory effects [1]. As such, CB_2 has been indicated as a potential therapeutic target in chronic inflammatory conditions including osteoporosis, inflammatory bowel disease, and neurodegenerative diseases involving neuroinflammation [1,2]. Due to its largely peripheral and non-neuronal distribution, activation of CB_2 is not associated with the psychotropic effects of cannabis, further supporting it as a promising therapeutic target.

GPCRs have traditionally been considered to primarily function at the cell surface, where their activation by extracellular ligands results in the transduction of downstream signals. Following either ligand-induced or constitutive activation, the majority of GPCRs desensitise and are subsequently internalised. CB_2 canonically couples to $G\alpha_{i/o}$ G proteins [3] and subsequent to activation has been demonstrated to internalise [4–7] though this has been suggested to be dependent upon the specific ligand [8] [6]. Post-endocytic trafficking is a critical contributor to the subsequent potential for re-sensitisation to receptor ligands, with CB_2 understood to be recycled back to the cell surface as opposed to degraded [4,5].

A range of GPCRs have also now been reported to also be expressed intracellularly in unstimulated cells, and activation by cell permeable ligands with initiation of non-canonical signalling has been observed for a number of these, with implications for downstream function [9,10]. This is also true for CB_2, as a number of studies have found that a considerable proportion of CB_2 is expressed intracellularly in both immortalised cell lines and human primary immune cells [4,6,11–14]. Two studies to date have reported the potential for signalling via intracellular CB_2, one indicating $G\alpha_q$ coupling from CB_2 in endolysosomes [11] and the other inferring intracellular signalling in rat medial prefrontal cortex pyramidal neurons based on predominant intracellular CB_2 expression and timing differences of signalling onset depending on whether ligands were applied extracellularly or intracellularly [14].

Intracellular GPCR expression has also been associated with abnormal signalling and trafficking, in particular with relation to receptors that require interaction with an accessory protein in order to be delivered to the cell surface, and naturally occurring receptor mutations that prevent cell surface expression. In the latter case, the interaction of cell-permeable ligands with intracellular receptors can act as “pharmacological chaperones” (also referred to as “pharmacoperones”) to facilitate receptor delivery to the cell surface and enable functional recovery [15,16]. This is hypothesised to be via facilitation of appropriate receptor folding and/or conformation

which enables subsequent progression through the secretory pathway [17]. Interestingly, surface expression of wild-type receptors can also be modulated via pharmacological chaperoning [18]. Signalling responses have also been implicated in the modulation of cell surface delivery of proteins, acting as a form of positive feedback with the effect of maintaining ongoing responsiveness [19,20].

Given the potential for differential signalling responses between subcellular receptor populations, regulation of the subcellular distribution of GPCRs is likely to be a critical determinant of functional outcome of GPCR activation. In this study, we undertook to further understand CB_2 intracellular trafficking and subcellular distribution. Herein we describe our findings that CB_2 ligands can act as pharmacological chaperones of newly synthesised CB_2, and that this trafficking pathway is regulated distinctly from basal and post-endocytic subcellular distribution.

2 Methods

2.1 Drugs and chemicals

CP 55,940, anandamide (AEA), 2-arachidonoyl glycerol (2-AG) were from Cayman Chemical (Ann Arbor, MI, USA). Isoproterenol, salbutamol, pertussis toxin (PTX), U73122, LY294002, GF109203X hydrochloride, monensin and cycloheximide (CHX) were from Sigma-Aldrich (St. Louis, MO). WIN 55,212-2 and HU308 were from Tocris Bioscience (Bristol, UK), and Δ^9tetrahydrocannabinol (Δ^9-THC) was from THC Pharm (Frankfurt, Germany). AM630 and SR144528 were kind gifts from Roche (Basel, Switzerland). Gallein was from Santa Cruz Biotechnology (Dallas, TX, USA) and brefeldin A (BFA) from BioLegend (San Diego, CA, USA).

2.2 Generation of stable cell lines and cell culture

HEK Flp-in-293 cells (Thermo Fisher Scientific, Waltham, MA; #R750-07) were stably or transiently transfected to express human (h)CB_2. This hCB_2 wild-type (wt) construct (hCB_2 wt), with an haemagglutinin (HA) tag and three thrombin cleavage sites (3TCS) appended at the N-terminus of the receptor, was assembled by overlap-extension PCR, using hCB_2 sequence from the cDNA Resource Centre (www.cdna.org, CNR0200000; 63Q single nucleotide polymorphism [21]) and synthetic DNA oligos for the tags (Integrated DNA Technologies, Coralville, IA), then ligated into pcDNA5/FRT vector (Thermo Fisher Scientific) via NheI and XhoI restriction sites using standard molecular biology techniques, and sequence verified (see also [22], pERK section). hCB_2 KK318-9EE ("KK mutant"), ETE339-41ATA ("ETE mutant") and truncation of the last 12 amino acids from the C-terminus (Δ12) were generated via site-directed mutagenesis utilising the Quikchange® approach (Stratagene, San Diego, CA, USA) with slight modifications and using KAPA HiFi polymerase (KAPA

107 Biosystems, South Africa). The HA-3TCS-hβ_2-AR pcDNA5/FRT (hβ_2-AR) plasmid was generated with an
108 analogous strategy as for hCB_2 wt (www.cdna.org, AR0B20TN00).

109 Cell lines stably expressing hCB_2 or hβ_2-AR plasmids were generated by co-transfecting the receptor-
110 containing plasmid with pOG44 (Thermo Fisher Scientific) to facilitate targeted integration into the FRT site of
111 the HEK Flp-in-293 cell line using Lipofectamine 2000 (Thermo Fisher Scientific). Hygromycin B (Thermo
112 Fisher Scientific) was used for initial selection of transfected cells (100 $\mu g \cdot mL^{-1}$) and subsequent routine
113 maintenance (50 $\mu g \cdot mL^{-1}$).The 3HA-hCB_1 construct and HEK cell line have been described previously [23].

114 All cell lines were maintained in high-glucose DMEM (HyClone, GE Healthcare Life Sciences, Chicago, IL,
115 USA) supplemented with 10% FBS (NZ-origin; Moregate Biotech, Brisbane, Australia) and appropriate
116 selection antibiotics, and incubated at 37°C in 5% CO_2 in a humidified atmosphere.

117 ***2.3 Immunocytochemistry and receptor trafficking assays***

118 Cells were seeded at a density of 45,000 cells/well (for stably expressing lines) or 30,000 cells/well (for cells
119 to be transiently transfected) in poly-D-lysine-treated (Sigma-Aldrich) clear 96-well plates (Nunc, Thermo
120 Fisher Scientific). For assays involving transient receptor expression, receptor constructs were transfected
121 approximately 24 hours post-seeding using Lipofectamine 2000 (Thermo Fisher Scientific), per a slightly
122 modified manufacturer's protocol.

123 Assays were carried out approximately 24 hours post-seeding for stable cell lines and 18-24 hours post-
124 transfection for transiently transfected cells. All drugs and reagents were prepared in high glucose DMEM
125 supplemented with 1 $mg \cdot mL^{-1}$ low endotoxin bovine serum albumin (BSA; ICPBio, Auckland, NZ; "assay
126 medium"). Prior to any antibody labelling or drug treatment, cells were equilibrated in assay medium for 30 min
127 at 37°C in 5% CO_2.

128 Two immunocytochemical approaches for measuring the influence of ligands on receptor cell surface
129 expression were utilised in this study (Fig. 1A). In "***Method A***", cell surface receptors are labelled with primary
130 antibody prior to drug treatment, and primary antibody remaining at the cell surface following drug treatment
131 is quantified. Because only receptors that were at the cell surface prior to drug stimulation can be labelled, this
132 method detects residual surface receptor expression, typically providing a direct measurement of receptor
133 internalisation. Cells were incubated with mouse monoclonal anti-HA (901503; BioLegend, San Diego, CA,
134 USA) diluted 1:500 in assay medium for 30 min at room temperature (RT). Cells were then washed with assay
135 medium and stimulated with vehicle or drug for the indicated time period at 37°C. At the conclusion of the drug

136 stimulation, plates were placed on ice for a minimum of 2 min to halt membrane trafficking and washed with
137 RT assay medium. Alexa Fluor 488-conjugated goat anti-mouse secondary antibody (Invitrogen; diluted 1:300
138 in assay medium) was then applied to cells and incubated for 30 min at 15°C (preventing further trafficking
139 [24,25]), prior to washing twice with assay medium and fixation (below).

140 In contrast, "***Method B***" labels cell surface receptors with primary antibody *after* drug treatment. Therefore, as
141 well as receptors that remain at the cell surface following drug stimulation, any receptors delivered to the cell
142 surface during stimulation will also be detected. Cells were first stimulated with vehicle or drug for the indicated
143 period of time at 37°C. At the conclusion of the drug stimulation, plates were placed on ice for a minimum of
144 2 min to halt membrane trafficking and washed with RT assay medium. Cells were then incubated with anti-
145 HA diluted 1:500 in assay medium for 30 min at 15°C (preventing further trafficking), then washed twice with
146 assay medium.

147 For both methods, cells were then fixed in 4% paraformaldehyde (PFA) at RT for 10 min and washed twice
148 with phosphate buffered saline (PBS). Cells labelled via *Method B* were then incubated with Alexa Fluor 488-
149 conjugated goat anti-mouse secondary (diluted 1:400 in immunobuffer: PBS with 0.2% Triton X-100 [PBS-T],
150 1% normal goat serum and 0.4 $mg \cdot mL^{-1}$ thiomersal [Merck, Darmstadt, Germany]), for 3 hours at RT or
151 overnight at 4°C, and washed with PBS-T. For both methods, cell nuclei were then labelled with Hoechst 33258
152 (Sigma-Aldrich) 8 $\mu g \cdot mL^{-1}$ in PBS-T.

153 Where total receptor expression was measured, drug stimulations and cell fixation were carried out as
154 described above but without any antibody labelling. When cell lines with stable receptor expression were
155 assayed, 90% methanol was applied for 10 min at -20°C, then removed and the plate allowed to air dry for
156 ~3 min before re-hydrating in PBS-T. Cells were then incubated with anti-HA diluted 1:2500 in immunobuffer
157 for 3 hours at RT or overnight at 4°C, washed with PBS-T, then labelled with secondary antibody and Hoechst
158 as above.

159 For confocal imaging to illustrate surface versus intracellular CB_2, cells were plated in chamber slides (BD
160 Biosciences, Franklin Lakes, NJ, USA) and processed for immunocytochemistry, generally as above. In brief,
161 live cells were cooled to 15°C and incubated with anti-HA then Alexa 488-conjugated secondary, fixed and
162 permeabilised, then re-probed with anti-HA, followed by Alexa 594-conjugated secondary and Hoechst stain.
163 Slides were mounted with AF1 antifadent (Citifluor, Hatfield, PA, USA).

164 ### *2.3.1 Cell surface receptor turnover*

165 For assays measuring receptor turnover at the cell surface, cells were incubated with anti-HA primary antibody
166 diluted 1:500 in assay medium for 30 min at RT. Cells were then stimulated with vehicle or 1 μM CP 55,940
167 for 3 hours at 37°C in the *continued* presence of anti-HA antibody. At the conclusion of the drug stimulation,
168 cells were fixed in 4% PFA, incubated with Alexa Fluor 488-conjugated goat anti-mouse secondary in
169 immunobuffer (with Triton X-100), and stained with Hoechst 33258 as above. The presence of anti-HA primary
170 throughout the drug stimulation, and the application of secondary antibody under membrane permeabilising
171 conditions, allowed the surface turnover of receptor to be detected (i.e. receptor that was delivered to and/or
172 internalised from the surface at any point throughout the drug stimulation).

173 ### *2.3.2 Thrombin strip*

174 In some experiments, proteolytic enzyme thrombin was used to cleave extracellular HA epitopes, thereby
175 preventing labelling of surface HA-tagged receptor with anti-HA primary antibody, but leaving intracellular HA
176 epitopes intact. At the appropriate point in the assay, thrombin (50 $U \cdot mL^{-1}$; Bio-Pharm Inc., Hatfield, AR) or
177 assay medium was applied to cells and incubated for 30 min at 37°C. Plates were placed on ice for a minimum
178 of 2 min and washed with the protease inhibitor phenylmethylsulfonyl fluoride (PMSF, 250 μM; Sigma-Aldrich)
179 to inactive thrombin. For experiments validating the effectiveness of the thrombin strip, cells were incubated
180 with mouse monoclonal anti-HA diluted 1:500 in assay medium for 30 min at 15°C, and washed twice with
181 assay medium to label any remaining HA epitopes at the cell surface. Cells were then fixed in 4% PFA. For
182 experiments measuring intracellular versus total receptor (with and without thrombin strip, respectively), cells
183 were methanol unmasked then anti-HA was incubated in immunobuffer as described above for total receptor
184 detection. For both experimental designs, secondary antibody and Hoechst labelling was then carried out as
185 described above.

186 ### *2.3.3 Inhibitors of signalling, trafficking, protein synthesis and monoacylglycerol lipase (MAGL)*

187 For trafficking assays utilising PTX, cells were seeded in half the usual volume of medium. ~5 hours later, PTX
188 (final concentration 100 $ng \cdot mL^{-1}$) or vehicle were prepared in medium and applied to the pre-plated cells. Cells
189 were exposed to PTX or vehicle for 16-20 hours prior to the start of the trafficking experiment.

190 Other inhibitors were pre-incubated at 2x their intended final concentration, after which CB_2 agonist or vehicle
191 was added which diluted the inhibitor to the 1x final concentration for the duration of the drug stimulation. Final
192 concentrations and pre-incubation times were: Gallein 10 μM, 30 min; U73122 1 μM, 30 min; LY294002

193 10 μM, 30 min; GF109203X 1 μM, 30 min; BFA 1 μg·mL^{-1}, 10 min; monensin 1 μM, 10 min; CHX 10 μg·mL^{-1},
194 10 min; JZL148 1 μM, 30 min.

195 ### *2.4 Image acquisition and analysis*

196 Assays utilising immunocytochemistry were quantified via automated image acquisition and analysis [5,26–
197 28]. Briefly, images from four sites per well were captured using a 10x objective on an ImageXpress Micro XLS
198 widefield microscope (Molecular Devices, Sunnyvale, CA) housed in the Biomedical Imaging Research Unit at
199 the University of Auckland. Analysis was carried out with MetaXpress (v6.5, Molecular Devices) or MetaMorph
200 (v7.10, Molecular Devices) software. User-defined thresholds were applied consistently within each
201 experiment to define the boundary between genuine staining and background ("staining of interest threshold"),
202 exclude brightly fluorescent debris if necessary, and to segment nuclei from background. The inbuilt 'Find
203 Spots' algorithm was used to count the number of cells per image. Receptor expression was then quantified
204 by integrated fluorescence intensity per cell [28] For all trafficking assays, receptor expression was normalised
205 to the vehicle-treated condition (100%). Anterograde trafficking was subsequently calculated by subtracting
206 measurements for *Method A* from *Method B*.

207 Confocal images were taken on a Leica TCS SP2 system with 63x objective lens, as described previously [29].

208 ### *2.5 Western Blotting*

209 Cells were seeded in 24 well plates and transiently transfected with hCB_2 wt, KK mutant, or benign plasmid
210 [27] using Lipofectamine 2000 (Thermo Fisher Scientific). Drugs and reagents were prepared, and cells
211 stimulated 18-24 hours post-transfection, as described in Section 2.3 for 3 hours. Plates were then placed on
212 ice for 2 min and washed with RT assay medium.

213 Cells were harvested in lysis buffer (150 mM NaCl, 1% Triton X-100, 50 mM Tris-HCl pH 8, cOmplete protease
214 inhibitor cocktail tablets [Roche]), incubated on ice for 30 min and centrifuged for 10 min at 4°C. Supernatants
215 were aspirated and diluted with 4x loading buffer (125 mM Tris-HCl pH 6.8, 50% glycerol, 4% sodium dodecyl
216 sulfate [SDS]), and protein concentrations quantified. Cell lysate concentrations were standardised in 1x
217 loading buffer with 0.001% bromophenol blue and heated for 30 min at 37°C. Lysates (15 μg per well) were
218 separated on a 4-12% pre-cast gel (Invitrogen) by electrophoresis, followed by semi-dry transfer to
219 polyvinylidene fluoride membranes. Membranes were air dried and rehydrated in methanol, rinsed, and
220 blocked in 5% non-fat milk (NFM) in 0.1 M Tris-buffered saline with 0.2% Triton X-100 (TBS-T) for 30 min at

221 RT. Mouse monoclonal anti-HA (901503; BioLegend) and rabbit polyclonal anti-glyceraldehyde 3-phosphate
222 dehydrogenase (GAPDH; ab9485; Abcam) diluted 1:1000 in 1% NFM/TBS-T were co-incubated for 3 hours at
223 RT or overnight at 4°C. Following three TBS-T washes, membranes were co-incubated with fluorescently
224 conjugated secondary antibodies (IRDye® 680LT goat anti-mouse [926-68020; LI-COR Biosciences, Lincoln,
225 NE] and IRDye® 800CW goat anti-rabbit [926-32211; LI-COR Biosciences]) diluted 1:20 000 in 1% NFM/0.01%
226 SDS/TBS-T for 3 hours at RT or overnight at 4°C. Membranes were then rinsed and left to air dry prior to
227 imaging.

228 Images were captured on an Odyssey® FC Imaging System (LI-COR Biosciences) in 700 nm and 800 nm
229 channels, and quantified using Image Studio (Lite; LI-Cor Biosciences). GAPDH and HA bands were
230 segmented using the shapes tool and integrated intensity above background obtained. In the anti-HA channel,
231 the corresponding HEK Flp-in wt (i.e. no CB_2) measurement was subtracted from the total signal for each
232 band/range of bands, and the remaining signal normalised to its respective GAPDH. Within each treatment
233 condition (i.e. lane), signals for each distinct band or range of molecular weights, were then normalised to the
234 total signal in the lane for that particular treatment condition to determine what proportion each band, or range
235 of molecular weights, contributed to total expression. Uncropped blot images were provided for peer review.

236 ***2.6 General analysis and statistics***

237 All graphs were prepared in GraphPad Prism (v10; GraphPad Software Inc., La Jolla, CA). Sigmoidal three-
238 parameter nonlinear regression concentration-response curves were fitted and parameters obtained ("span"
239 and $\log EC_{50}$) for independent experiments. Statistical analyses were performed on data from three to four
240 independent experiments using Sigmaplot™ v13.0 (Systat Software Inc., San Jose, CA, USA). The Shapiro-
241 Wilk test for normality and Brown-Forsythe test for equal variance were performed to verify the datasets were
242 appropriate for analysis with parametric statistical tests. Where a set of results did not pass either of these
243 tests, datasets were transformed ($\log_{10}$ or e^x) to change the nominal values of the sample distribution, and re-
244 tested. Following a pass result of $p > 0.05$, a Student's t-test, one-way ANOVA, or two-way ANOVA was carried
245 out as appropriate for the number of conditions and factors under comparison. A paired or repeated measures
246 design was used where appropriate. If a statistically significant difference ($p < 0.05$) was detected, the Holm-
247 Šídák [30] post-hoc test was used to test for significant differences within/between groups. p values are
248 indicated graphically as: * < 0.05, ** < 0.005, *** < 0.001.

249

250 **3 Results**

251 ***3.1 Agonist stimulation induces concurrent CB_2 internalisation and anterograde trafficking***

252 The effect of a 3 hour stimulation with CP 55,940 on cell surface expression of both stably- and transiently-
253 expressed hCB_2 wt was investigated via two immunocytochemical labelling methods that we refer to herein as
254 *Method A* and *Method B* (Fig. 1A). When surface CB_2 was labelled with antibody *prior to* agonist stimulation
255 (*Method A*), an agonist concentration-dependent decrease in CB_2 surface expression was observed, which is
256 indicative of agonist-induced internalisation (Fig. 1B, Table 1). Potency was approximately equivalent between
257 stable and transient CB_2 expression ($p > 0.05$). However, the proportional extent of internalisation was greater
258 in the stably-expressing cells, whereby ~20% more of the starting surface population was internalised
259 ($p = 0.004$). This was likely a consequence of the greater surface (and overall) CB_2 expression level in the
260 transiently-expressing cells (surface CB_2: 8.6 [±1.3] times that of stably-expressed; total CB_2: 101 [±29] times
261 that of stably-expressed), and consistent with a prior report [8].

262 When surface CB_2 was labelled *following* CP 55,940 stimulation via *Method B* (monitoring net surface
263 expression), surface CB_2 expression was reduced by CP 55,940 concentrations in the region of the EC_{50} for
264 internalisation (Fig. 1C). Conversely, at greater concentrations a lesser, or lack of, change in surface CB_2 was
265 observed in both expression conditions. Unlike *Method A*, which measures the proportion of initial surface CB_2
266 remaining, *Method B* is a measure of net surface expression. It is apparent from Fig. 1B that the receptors
267 initially on the cell surface and internalised by CP 55,940 remain internalised. A prior study utilising *Method A*
268 has validated that the antibody used to label cell surface CB_2 remains bound to the receptor, with no detectable
269 degradation after a 4 hour agonist stimulation, and can be detected to recycle when agonist is replaced by
270 inverse agonist [5]. Therefore, plain interpretation of the discrepancy between the findings from labelling
271 *Methods A* and *B* (Fig. 1B and C) is that, despite cell surface CB_2 undergoing internalisation, CP 55,940 can
272 *also* stimulate delivery of non-cell surface-derived CB_2 to the plasma membrane. We hypothesised that the
273 source of the delivered receptors may be the "intracellular pool" described in earlier studies. Indeed, in our
274 cells approximately 50-70% of overall CB_2 expression was observed to be intracellular, as determined by
275 comparing total CB_2 expression with and without enzymatic cleavage of the surface HA tag and was evident
276 in confocal imaging (Fig. 1F and G).

277 A reduction in surface expression in *Method A* is indicative of receptor internalisation, whereas *Method B*
278 measures net surface expression which is a product of both internalisation and delivery of new receptors to
279 the cell surface. The difference between these methods therefore reflects stimulated anterograde delivery of

280 CB_2 to the cell surface (Fig. 1D, Table 1). The potency of CP 55,940-induced CB_2 anterograde trafficking at a
281 3 hour time point, was approximately 30- to 100-fold lower than that for internalisation. The maximal extent of
282 stimulated cell surface re-population was equivalent to around 60-80% of cell surface expression in
283 unstimulated cells (Fig. 1D, Table 1).

284 Total cellular CB_2 expression was also monitored following CP 55,940 stimulation. This revealed increases in
285 expression at CP 55,940 concentrations that induced anterograde trafficking of CB_2 in both expression
286 conditions (Fig. 1E). The maximal increase in expression measured was only significantly different from vehicle
287 when hCB_2 wt was transiently expressed (Fig. 1E; $p < 0.001$). In addition, slight decreases in total expression
288 were observed at intermediate CP 55,940 concentrations in the stably-expressing line, but not with transient
289 hCB_2 wt expression.

290 Despite transient expression producing greater overall CB_2 expression per cell than stable expression, findings
291 between stably- and transiently-expressed CB_2 in Fig. 1 were largely similar, validating the use of both
292 transiently- and stably-expressing cells for further characterisation of these processes.

293 To further investigate the time-dependence of the CB_2 trafficking phenotype, a time course over 6 hours was
294 carried out in response to 1 μM CP 55,940 (a concentration that induced a pronounced degree of anterograde
295 trafficking at 3 hours). When *Method A* was used, the application of primary antibody was staggered so that
296 constitutive internalisation could be measured over the time course, as seen in the "vehicle" condition of Fig.
297 2A. Approximately 70% of surface CB_2 internalised in response to CP 55,940 within 0.5 hours, and the residual
298 surface expression remained unchanged over the remaining time course. When net surface expression was
299 measured (*Method B*), a reduction relative to vehicle was observed at 0.5 and 1 hour, followed by no change
300 and/or an increase at later time points (Fig. 2B). Subtraction of *Method A* (internalisation) from *Method B* (net
301 surface expression) to reveal any anterograde trafficking/surface delivery of hCB_2 wt allowed measurement of
302 constitutive surface delivery in the vehicle condition, and the combination of constitutive and ligand-induced
303 surface delivery in the CP 55,940 condition (Fig. 2C). The difference between the vehicle and CP 55,940 traces
304 therefore corresponds to CP 55,940-induced surface delivery. Anterograde trafficking of hCB_2 wt in response
305 to CP 55,940 was significantly different from vehicle at all time points > 1 hour ($p = 0.005$, < 0.001, < 0.001
306 respectively), indicating that this phenotype is detectable following a lag time of at least 1 hour. CP 55,940-
307 induced surface delivery continued at a steady rate over the remainder of the time course.

308 To explore whether CP 55,940-induced anterograde trafficking was particular to CB_2, concentration responses
309 using the labelling methods described above were carried out in HEK293 cells stably expressing HA-tagged

310 CB_1 or hβ_2-AR. As CP 55,940 is a full agonist at CB_1 (in addition to CB_2), and β_2-AR is a well-characterised
311 recycling receptor, these receptors are appropriate controls in this context. The hβ_2-AR-specific ligands
312 salbutamol and isoproterenol induced a concentration-dependent decrease in surface hβ_2-AR expression, and
313 CB_1 was similarly internalised in response to CP 55,940 (Fig. 3A and B). In both cases, the two labelling
314 methods produced interchangeable concentration response curves with no evidence of ligand-stimulated
315 anterograde trafficking at any ligand concentration. In addition, when CP 55,940 was applied to β_2-AR at
316 concentrations shown to either internalise or stimulate surface delivery of hCB_2 wt, (i.e. 10 nM and 1 μM,
317 respectively), surface receptor expression was equivalent between labelling conditions (Fig. 3C). This
318 indicates that CP 55,940-induced anterograde trafficking is CB_2-specific, and not an artefact of the labelling
319 methods employed or a result of a general effect on receptor trafficking in the HEK cell line, nor a result of
320 modified control of the constitutive CMV promoter (as β_2-AR and CB_2 were both expressed under the CMV
321 promoter).

322 ***3.2 A di-lysine 'KK' motif is required for basal surface delivery of CB_2 but not CP 55,940-induced***
323 ***anterograde trafficking***

324 CB_2 has *ExE* and *KK* motifs in its cytoplasmic (C-terminal) tail, which have been shown to modulate secretory
325 pathway trafficking in other GPCRs [31–34]. CB_2 constructs containing mutations to these motifs (ETE339-
326 41ATA and KK318-9EE), as well as a truncated Δ12 mutant (lacking the last 12 residues of the CB_2 C-terminal
327 tail, 349-360) were screened to determine their effects on internalisation and net surface expression in
328 response to CP 55,940 relative hCB_2 wt. The ETE and Δ12 mutants had similar basal surface expression and
329 trafficked equivalently to wt in response to CP 55,940 (Fig. 4A and B). In contrast, mutation of the KK motif
330 abolished basal surface expression of CB_2, indicating that this motif influences typical receptor trafficking or
331 synthesis. Despite this, exposure to CP 55,940 stimulated surface expression of the KK mutant. Total
332 expression levels of all CB_2 mutants were greater than that of hCB_2 wt, indicating that none of these mutations
333 affected overall receptor synthesis and/or turnover (Fig. 4C).

334 Assays measuring the effect of CP 55,940 on the surface expression of transiently and stably expressed KK
335 mutant receptor were performed (analogous to those for hCB_2 wt in Fig. 1). As expected, no basal surface
336 expression of the KK mutant was detected when receptor was labelled prior to agonist stimulation (*Method A*,
337 Fig. 5A). However, a CP 55,940 concentration-dependent increase in net surface expression (*Method B*) was
338 observed, and this was equivalent between transfection conditions (Fig. 5B). The ultimate extents of CP 55,940
339 induced-surface delivery were equivalent between hCB_2 wt and KK mutant, but the effect was ~1 log unit more

340 potent for hCB_2 wt (Fig. 1D versus 5C; Table 1 versus Table 2). As with hCB_2 wt, total expression of the KK
341 mutant increased at CP 55,940 concentrations that also induced anterograde trafficking (Fig. 5D).

342 Lack of basal surface expression of the KK mutant could be due to either impaired delivery to the cell surface,
343 or efficient surface delivery followed by rapid constitutive internalisation. To clarify this, we measured surface
344 turnover of hCB_2 wt versus the KK mutant during a 3 hour incubation in media (with vehicle) or CP 55,940 (Fig.
345 5E-F). "Surface turnover" was assessed by incubating cells in the continued presence of anti-HA, such that
346 receptor trafficking via the cell surface at any point during the assay would bind antibody. Secondary antibody
347 was then applied under permeabilising conditions to detect anti-HA bound receptor anywhere in the cell, even
348 if it had subsequently internalised. Stimulation of hCB_2 wt with CP 55,940 enhanced surface turnover
349 compared with vehicle, consistent with CP 55,940-induced surface delivery. The equivalent was true for the
350 KK mutant, which had a considerable amount of antibody bound in response to CP 55,940 stimulation. In
351 contrast, no antibody labelling could be detected for KK mutant-expressing cells incubated with vehicle only,
352 indicating lack of constitutive receptor delivery to the cell surface over 3 hours (Fig. 5E and F). Non-specific
353 antibody uptake (in untransfected cells) was below detectable limits (Fig. 5E). Combined with previous findings,
354 this indicates that in unstimulated cells the KK318-9EE mutation prevents constitutive CB_2 delivery to the
355 plasma membrane.

356 ***3.3 hCB2 wt and KK mutant possess the same maturation states in differing proportions, with***
357 ***maturation states altered by agonist stimulation***

358 From this data, as well as prior findings in other receptors [31,32,34], we hypothesised that the KK318-9EE
359 mutation might be inhibited from traversing and/or exiting the secretory pathway basally, whereas stimulation
360 with CP 55,940 seems to release this blockade. Western blotting revealed numerous molecular weight species
361 in both CB_2 wt and KK mutant lysates, of which the three most prominent and size-resolved bands were ~35
362 kDa, ~40 kDa, and ~67 kDa, with species of varying size also evident between ~40 and ~55 kDa, and above
363 ~67 kDa (Fig. 6A). As the predicted molecular weight of unmodified CB_2 wt and KK mutant constructs is ~42.5
364 kDa, the ~35 kDa species likely represents immature CB_2. Indeed, receptor species have previously been
365 observed to be smaller than their predicted size via western blot [29,35,36]. The ~40 kDa species observed
366 here is therefore likely to be a more mature form of CB_2, based on a prior report of a 5 kDa difference between
367 mature and de-glycosylated human CB_2 [37], while the >40 to ~55 kDa forms might have more complex
368 glycosylation or other post-translational modifications, and/or be complexed with small interacting proteins.
369 The ~67 kDa and larger species might reflect CB_2 homodimer (previously shown to be ~87 kDa in [37]) or CB_2

370 complexed with other interacting protein(s). As expected, no anti-HA staining was detected in the HEK Flp-in
371 wt control, indicating specificity for HA-tagged CB_2.

372 Blots were analysed quantitatively for proportional expression of molecular weight species within each receptor
373 type and treatment condition (Fig. 6B). The smallest ~35 and ~40 kDa bands represented fairly equivalent
374 proportions of total receptor expression between wt and KK mutant CB_2, and were unchanged by CP 55,940.
375 The >67 kDa and ~67 kDa species made up a larger proportion of KK mutant relative to CB_2 wt in vehicle-
376 treated cells (~41% versus ~3f4% and ~20% versus 12%, respectively), though only the latter was significantly
377 different ($p = 0.001$). Conversely, species ranging from ~40 to 55 kDa were more prominent in CB_2 wt than in
378 the KK mutant, comprising ~27% of total CB_2 wt expression, but ~15% of KK mutant ($p = 0.021$). CP 55,940
379 stimulation appeared to reduce the proportional expression of the ≥67 kDa species for both WT and KK mutant,
380 with significant differences for all ($p = 0.001$ - 0.032) except CB_2 wt >67 kDa species. In an inverse shift, the
381 proportional expression of species ranging from ~40 to 55 kDa increased in response to CP 55,940 for both
382 receptors ($p = 0.017$ for CB_2 wt, $p = 0.027$ for KK mutant).

383 ***3.4 CP 55,940-induced anterograde trafficking of CB_2 does not require common signalling***
384 ***pathways***

385 We hypothesised that a mechanism involving CB_2 signalling may be a feedback mechanism stimulating the
386 CP 55,940-induced CB_2 cell surface delivery observed. To test this, we measured residual starting surface
387 and net surface expression concentration response curves in response to CP 55,940 in the absence and
388 presence of various signalling inhibitors: irreversible $G\alpha_{i/o}$ and $G\beta\gamma$ inhibitor PTX, $G\beta\gamma$ inhibitor gallein,
389 phospholipase C [PLC] inhibitor U73122, phosphoinositide 3-kinase [PI3K] inhibitor LY249002, and protein
390 kinase C [PKC] inhibitor GF109203X.

391 CP 55,940-stimulated CB_2 internalisation potency and efficacy were unaffected by the signalling inhibitors
392 ($p > 0.05$; Fig. 7A and Table 3). The signalling inhibitors had no significant effects on CP 55,940-stimulated
393 surface delivery of hCB_2 wt or KK mutant ($p > 0.05$; Fig. 7C-D, Table 3). Cell morphology and number were
394 also unaffected by signalling inhibitors (data not shown).

395 ***3.5 CP 55,940-induced anterograde trafficking of CB_2 is blocked by inhibitors of Golgi export,***
396 ***vesicle acidification, and protein synthesis***

397 To further characterise CP 55,940-stimulated surface delivery of CB_2, the effect of inhibitors of receptor
398 trafficking and protein synthesis were investigated. BFA is a macrocyclic lactone that disrupts the Golgi and

399 prevents protein secretion to the plasma membrane [38]. Monensin is an inhibitor of vesicle acidification and
400 therefore of receptor trafficking to the cell surface [39]. CHX inhibits protein synthesis at the translational level
401 [40] and was included to determine whether new protein synthesis was required for this phenotype to occur.

402 These inhibitors did not influence CB_2 internalisation (*Method A*) in response to CP 55,940 ($p > 0.05$; Fig. 8A,
403 Table 3). However, co-administration of these inhibitors, did influence net surface expression (*Method B*) and
404 the resulting extent of anterograde trafficking in response to CP 55,940 (Fig. 8B-D).

405 Treatment with BFA reduced CB_2 wt net surface expression in response to CP 55,940, producing a
406 concentration-response curve in this labelling condition (Fig. 8B) with equivalent efficacy and potency to that
407 when measuring internalisation alone (Fig. 8A). CP 55,940-induced anterograde trafficking was therefore
408 found to be abolished when BFA was present (Fig. 8C). This was also apparent with the KK mutant where
409 CP 55,940 did not stimulate CB_2 wt surface delivery in the +BFA condition (Fig. 8D).

410 The presence of monensin similarly attenuated CB_2 wt net surface expression in response to CP 55,940 (Fig.
411 8B), and CP 55,940-induced anterograde trafficking was partially blocked by this inhibitor, wherein a ~50%
412 reduction in efficacy relative to the vehicle-treated condition was observed (Fig. 8C, Table 3; $p = 0.018$). This
413 was evident with the KK mutant also, but to an even greater degree, where CP 55,940-induced surface delivery
414 was completely blocked (Fig. 8D, Table 3).

415 Inhibiting protein synthesis with CHX treatment also resulted in a significant decrease in net surface expression
416 of CB_2 wt following CP 55,940 stimulation, and partial blockade of the stimulated surface delivery phenotype,
417 reducing its efficacy by ~60% when compared to CP 55,940 plus inhibitor vehicle (Fig. 8B & C, Table 3;
418 $p = 0.026$). Again, this was recapitulated with the KK mutant, where the efficacy of CP 55,940-induced CB_2 wt
419 anterograde trafficking was reduced to ~15% of the CP 55,940 plus inhibitor vehicle response (Fig. 8D, Table
420 3).

421 A significant reduction in CB_2 basal total expression was found in the presence of CHX ($p = 0.001$) and BFA
422 ($p = 0.010$), but not monensin (Fig. 8G). For the KK mutant, all inhibitors produced a significant reduction in
423 basal total expression relative to vehicle ($p = 0.002$ for BFA, $p = 0.043$ for monensin, $p < 0.001$ for CHX).
424 Additionally, cell numbers were consistent between conditions, indicating that none of the inhibitors had a
425 gross effect on cell health/viability ($p > 0.05$; Fig. 8H). When normalised to their respective CP 55,940 vehicles,
426 CB_2 wt total expression plus inhibitor vehicle was slightly reduced in response to intermediate concentrations
427 of CP 55,940, but a lesser/no change was observed at higher concentrations (Fig. 8E). The presence of

428 monensin resulted in an increase in CB_2 wt total expression, reaching a maximal ~30% above CP 55,940 plus
429 vehicle, but this was not statistically significant ($p > 0.05$). Co-incubation with BFA significantly increased CB_2
430 wt total expression at concentrations of CP 55,940 that would typically induce CB_2 wt anterograde trafficking,
431 reaching a maximum efficacy above CP 55,940 plus vehicle of ~85%, $p = 0.013$). Conversely, when CHX was
432 present CP 55,940 decreased total CB_2 wt expression ($p = 0.036$). KK mutant total expression data similarly
433 showed a slight increase in total expression in response to CP 55,940 plus vehicle, and this was further
434 increased in the presence of BFA, however this was not significant ($p > 0.05$). CHX and monensin similarly did
435 not affect KK mutant total expression in response to CP 55,940 ($p > 0.05$).

436 ***3.6 CB_2 anterograde trafficking is induced by cannabinoid agonists, antagonists, and inverse***
437 ***agonists***

438 The data presented above suggests that CP 55,940-induced anterograde trafficking is not signalling-mediated,
439 involves Golgi trafficking, requires new protein synthesis, and is specific to CB_2. In combination with the
440 lipophilic nature of CP 55,940 (and cannabinoids in general) and the CP 55,940-mediated changes observed
441 in the western blots, the evidence so far is consistent with CP 55,940-stimulated anterograde trafficking being
442 due to pharmacological chaperoning. As pharmacological chaperoning of GPCRs has previously been
443 observed in response to both agonists and inverse agonists [41,42], we investigated whether other CB_2
444 ligands, including inverse agonists, had the same effect as CP 55,940.

445 Trafficking assays were carried out in response to a panel of CB_2 agonists using the aforementioned labelling
446 methods (*Methods A* and *B*). The ligands chosen were structurally diverse and spanned various cannabinoid
447 classes. Synthetic cannabinoids HU308 and WIN 55,212-2 all internalised CB_2 wt when labelled *prior* to drug
448 stimulation (*Method A*, Fig. 9A-B, Table 4). CB_2 wt internalisation was not observed in response to the
449 phytocannabinoid Δ^9-THC (Fig. 9C). Endocannabinoids AEA and 2-AG both internalised CB_2 wt when labelled
450 via *Method A*, with AEA internalising to a lesser extent (Fig. 9D and E, Table 4). As these ligands possess a
451 wide range of affinities for CB_2, significant differences in internalisation EC_{50s} were expected, and this was
452 accordingly observed ($p < 0.001$). In regard to efficacy, significant differences were observed between AEA
453 vs. 2-AG and CP 55,940 ($p = 0.016$ and $p = 0.037$, respectively), and WIN 55,212-2 vs. 2-AG and CP 55,940
454 ($p = 0.007$ and $p = 0.016$). As Δ^9-THC did not internalise CB_2 wt, it was not included in this statistical analysis.

455 When labelled *following* drug stimulation (*Method B*), the synthetic cannabinoids induced a response similar
456 to CP 55,940, whereby CB_2 wt was internalised at lower agonist concentrations, but at greater concentrations
457 net surface expression was unchanged or increased (Fig. 9A-B). Despite not internalising CB_2 wt, Δ^9-THC

458 increased net surface expression in a concentration-dependent manner, reaching a maximal efficacy of ~160%
459 above vehicle (Fig. 9C). AEA produced a similar phenotype to the synthetic cannabinoids when labelled via
460 *Method B* (Fig. 9D). Conversely, 2-AG internalised CB_2 in a concentration-dependent manner, producing
461 concentration-response curves with equivalent efficacy (40.1 [± 2.5] vs. 31.9 [± 5.69]) and potency (6.13 [±
462 0.20] vs. 6.08 [± 0.17]) in both labelling conditions (Fig. 9E). A possible explanation for 2-AG not inducing CB_2
463 anterograde trafficking is that it may be degraded and therefore unable to interact with intracellular CB_2. To
464 address this, trafficking assays with 2-AG were carried out in the presence and absence of JZL184, an inhibitor
465 of monoacylglycerol lipase (MAGL, the metabolising enzyme that 2-AG is primarily degraded by). CB_2 wt
466 internalisation in response to 2-AG was unaffected by JZL184 ($p > 0.05$), and no anterograde trafficking was
467 detected in the presence of JZL184 (Supplementary Fig. 1).

468 For the panel of CB_2 agonists, ligand-induced anterograde trafficking was calculated by subtracting the surface
469 expression detected via labelling *Method A* from the surface expression detected via labelling *Method B*. As
470 seen in Fig. 9F and Table 4, the above ligands induced anterograde trafficking of CB_2 wt with varying
471 potencies, which is unsurprising given the range of internalisation potencies observed. While most of the
472 ligands screened induced anterograde trafficking of CB_2 wt to similar extents as CP 55,940 (~55-80% of
473 starting surface expression), Δ^9THC stimulation produced a greater efficacy of ~160%, whereas 2-AG did not
474 induce this phenotype at all. To compare the propensity of each ligand to induce CB_2 anterograde trafficking,
475 these concentration-response curves were re-plotted on the x-axis such that each ligand's own internalisation
476 EC_{50} was subtracted from each measured concentration (Fig. 9G). If the resulting internalisation-adjusted EC_{50}
477 for a compound were 0, this would indicate its propensity to induce anterograde trafficking was be equivalent
478 to that of internalisation. If the internalisation-adjusted EC_{50} were > 0, the propensity of the compound to induce
479 anterograde trafficking would be lesser than that for internalisation. This calculation therefore allows
480 comparison between ligands independent of internalisation potency. CP 55,940 was also included in this
481 analysis. As Δ^9-THC did not internalise hCB_2 wt and the anterograde trafficking EC_{50} for AEA could not be
482 measured reliably, these ligands were not included in the statistical analysis (Table 4) though, when plotted,
483 AEA qualitatively trended toward having the highest potency for anterograde trafficking relative to
484 internalisation EC_{50} of the ligands tested (Fig. 9G). HU308 qualitatively trended toward having lower relative
485 potency for hCB_2 wt anterograde trafficking than CP 55,940 and WIN 55,212-2, but no statistically significant
486 difference between these ligands was found ($p = 0.55$).

487 The above trafficking assays were also carried out in response to CB_2-selective inverse agonists, AM630 and
488 SR144528. When CB_2 wt was labelled *prior* to inverse agonist simulation, both inverse agonists produced a

489 concentration-dependent increase in staining relative to vehicle (indicative of inhibiting constitutive
490 internalisation) with equivalent potencies and similar efficacies (Fig. 10A and B, Table 4). When CB_2 wt was
491 labelled *following* inverse agonist stimulation, concentration-dependent increases in surface expression were
492 again measured in response to AM630 and SR144528, but to much greater extents (Fig. 10A and B, Table 4).
493 The efficacies produced here are also considerably larger than were produced by agonists, as seen when
494 compared to CP 55,940 (Fig. 10A and B, grey line).

495 To confirm that the inverse agonist-induced increases in CB_2 wt surface expression observed in Fig. 10A and
496 B, were not only a result of the stabilisation of existing surface receptors and/or the prevention of constitutive
497 degradation, trafficking assays in AM630 and SR144528 were carried out with the KK mutant. Surface receptor
498 expression was labelled *following* drug stimulation (*Method B*), and 1 μM CP 55,940 was included for
499 reference. Indeed, surface expression of the KK mutant was induced in response to both inverse agonists,
500 reaching a maximal efficacy ~110% greater than that induced by CP 55,940 for AM630, and ~80% greater for
501 SR144528, and confirming that these ligands are inducing CB_2 anterograde trafficking (Fig. 10C and D, Table
502 4). Inverse agonist-induced anterograde trafficking of CB_2 was ~1 log unit more potent at CB_2 wt vs. the KK
503 mutant for AM630, and ~1.5 log units more potent at CB_2 wt for SR144528. Trafficking summary parameters
504 for all ligands in this section are presented in Table 4.

505 **4 Discussion**

506 Herein, we have presented evidence that CB_2 surface expression can be stimulated by application of lipophilic
507 CB_2 agonists and inverse-agonists that likely act as pharmacological chaperones. As well, we report that a di-
508 lysine (KK) motif in the C-terminal tail is required for constitutive, but not chaperoned, delivery of CB_2 to the
509 cell surface.

510 Initially studying CP 55,940 as a prototypic CB_2 agonist, pharmacological chaperoning was demonstrated to
511 be particular to CB_2 as this was not observed for CB_1 or B_2AR. These experiments also confirmed that CP
512 55,940-induced CB_2 surface delivery was not due to modulation of the CMV promoter, nor an artefact of the
513 labelling methods/antibodies employed. Furthermore, in the presence of BFA to block release of CB_2 from the
514 secretory pathway, a treatment used previously to attenuate pharmacological chaperoning of other GPCRs
515 [43,44], equivalent internalisation responses were measured whether antibody was applied before (*Method A*)
516 or after (*Method B*) drug stimulation. This again validated that CB_2 internalisation observed utilising *Method A*
517 is not an artefact of live cell antibody labelling. The potential for CB_2-mediated signalling to contribute CP
518 55,940-induced surface delivery was ruled out by the lack of effect of a panel of signalling pathway inhibitors.

519 Providing further evidence for a pharmacological chaperone effect, at the same time as BFA blocked agonist-
520 induced CB_2 cell surface delivery, it considerably enhanced the agonist-induced increase in total expression.
521 This indicates that CP 55,940 has a positive effect on CB_2 expression stability prior to exit from the secretory
522 pathway, likely preventing degradation by quality control machinery [16]. Furthermore, these observations
523 imply that when BFA is *not* present, increases in surface and total expression in response to CP 55,940 arise
524 primarily from increased receptor stability in the secretory pathway, rather than post-delivery stabilisation at
525 the plasma membrane or prevention of post-endocytic degradation.

526 Interestingly, agonist-stimulated CB_2 surface delivery was partially blocked by the protein synthesis inhibitor
527 CHX. This implies that the majority of chaperoned CB_2 is not derived from the pre-existing intracellular pool.
528 Instead, chaperoning ligand needs to be present at a certain stage of CB_2 synthesis or maturation to be able
529 to promote delivery to the cell surface. This is also consistent with time course data, where there is an initial
530 lag time of at least one hour before a significant increase in CB_2 anterograde trafficking in response to
531 CP 55,940 is observed. Although CHX (as a broad spectrum protein synthesis inhibitor) could have blocked
532 anterograde receptor trafficking via reducing expression of chaperone proteins, this seems unlikely as the half
533 times for relevant chaperone proteins are reportedly in the scale of multiple hours [45,46]. These conclusions
534 from experiments with CHX and BFA parallel earlier findings for the delta opioid receptor (DOR), wherein a
535 large proportion of DOR was found not to be delivered to the cell surface and was instead proteasomally
536 degraded, but application of cell permeable antagonist could prevent this degradation and instead promote
537 cell surface delivery [42].

538 Early reports of GPCR pharmacological chaperoning focused on disease-causing mutations with low basal
539 cell surface expression that could be rescued by application of lipophilic receptor ligands [16]. While we are
540 not aware of any naturally occurring or disease-associated SNPs or mutations that markedly alter CB_2 surface
541 expression [21], we tested whether motifs in the C-terminal tail implicated in trafficking of other GPCRs may
542 be relevant for CB_2. Neither ETE339-41ATA nor truncation of the last 12 C-terminal residues had a measurable
543 effect on CB_2 trafficking. However, the KK318-319EE mutation inhibited all basal surface expression, despite
544 having similar total expression to wild-type CB_2. The role of the 'KK' motif can be context-dependent as it has
545 been reported to be an ER *retention* motif in metabotropic glutamate receptor 1b (mGluR1b) and some non-
546 GPCRs [31], but was important for surface expression of angiotensin II type 1 receptor (AT_1R;[34]) and bitter
547 taste receptor 4 [32], consistent with our observations here for CB_2. Antibody "feeding" experiments clarified
548 that the lack of CB_2 surface expression was due to lack of receptor delivery to the cell surface, rather than
549 rapid internalisation. Interestingly, KK318-9 is conserved between human and rodent CB_2, despite

550 considerable heterogeneity between the C-terminal tail sequences [47]. Only limited data is available on the
551 specific role of the KK motif in GPCR trafficking, but this has been suggested to interact with tubulin, which
552 might explain prevention of basal surface trafficking [34]. However, in strong support of the pharmacological
553 chaperoning hypothesis, CP 55,940 concentration-dependently "rescued" cell surface expression of the CB_2
554 KK318-9EE mutant. This implies that either pharmacological chaperoning by CB_2 ligands can divert CB_2 to be
555 delivered to the cell surface via a different mechanism from basal wt receptor delivery that is not dependent
556 on an intact KK motif, or that the KK318-9EE mutation introduces a 'gain of function' retention of CB_2 in the
557 secretory pathway that is reversed by chaperoning to enable CB_2 delivery to the cell surface.

558 A hallmark of pharmacological chaperoning in other GPCRs is a shift in receptor maturation state from
559 immature to mature species with chaperoning, as observed via western blotting (e.g. [42,48]). Here, we find
560 that basally a considerable population of CB_2 resolves in a ~67 kDa band, with additional species at a range
561 of larger sizes (perhaps complexed with chaperone proteins) and that the KK mutant has a larger proportion
562 in these species in comparison with wt. In response to CP 55,940 stimulation, the relative proportion of these
563 large complexes decreased and an increase in ~40 to ~55 kDa species was observed for both CB_2 wt and KK
564 mutant, which likely corresponds to the receptor being released from larger complexes and/or undergoing
565 post-translational modifications then being delivered to the cell surface. Interestingly, the proportions of ~35
566 and 40 kDa (likely immature) species were similar between CB_2 wt and KK mutant and unaffected by CP
567 55,940 stimulation, perhaps representing the intracellular pool.

568 Importantly, a panel of diverse CB_2 ligands – both agonists and inverse-agonists – were found to act as CB_2
569 pharmacological chaperones. Agonists HU308, WIN 55,212-2, AEA and 2-AG all internalised CB_2 wt, with
570 partial efficacy for WIN 55,212-2 and AEA being consistent with literature showing partial agonism for these
571 ligands in β-arrestin 2 recruitment [22,49]. Δ^9-THC did not induce CB_2 internalisation, which was consistent
572 with a prior-reported lack of β-arrestin recruitment [49,50]. Despite this, Δ^9-THC did engage with CB_2 as it
573 stimulated cell surface expression, and to a greater overall extent than CP 55,940 and the other agonists
574 tested, raising the possibility that a contributing mechanism to the immunomodulatory effects of cannabis may
575 be via enhancing CB_2 expression, after which endocannabinoids might induce greater effects. When the
576 potency of ligand-induced CB_2 anterograde trafficking was assessed relative to each agonist's internalisation
577 potency, no significant differences were observed between CP 55,940, HU308, and WIN 55,212-2. This
578 suggests that these ligands all have a similar propensity to induce CB_2 anterograde trafficking relative to their
579 ability to induce internalisation, with potencies ~75- to 200-fold lower than that for internalisation – this shift
580 perhaps being related to the lag time prior to onset of stimulated anterograde trafficking. While a reliable EC_{50}

could not be determined for AEA (as no plateau was observed), this qualitatively appeared to be the most potent of all the ligands screened for inducing anterograde trafficking. Despite acting as a full agonist for internalisation, 2-AG did not stimulate anterograde trafficking within the range of concentrations tested after 3 hours of stimulation. We verified this was unlikely to be due to enzymatic degradation of 2-AG during the assay via inclusion of a MAGL inhibitor. However, of the ligands tested 2-AG had the lowest potency for inducing internalisation and, based on relative ligand-stimulated anterograde trafficking potencies observed for most ligands (other than AEA), the highest concentration applied might not have been sufficient to produce chaperoning even if 2-AG has the potential to act in a similar way as the other agonists.

Inverse agonists AM630 and SR144528 increased surface expression of hCB_2 wt, which was consistent with previous studies [4,5]. These also induced CB_2 KK mutant surface expression, indicating that the increase in wild-type CB_2 surface expression was likely a result of both inhibition of constitutive internalisation and stimulated anterograde trafficking. These findings are also further evidence that the stimulated anterograde trafficking phenotype is not induced by agonist signalling and likely results from pharmacological chaperoning.

A limitation of our study is that experiments were performed in a heterologous expression system. It will be important to verify the ligand-induced anterograde trafficking phenotype in cells endogenously expressing CB_2, and investigate both the acute and long-term functional consequences. This may be challenging due to widely-reported poor reliability of anti-CB_2 antibodies [51–53] and because alternative ligand-based methods, such as radioligand binding or fluorescent ligand binding, are unlikely to be practical for validating this trafficking phenotype due to ligand competition issues. Furthermore, while other studies investigating pharmacological chaperoning of GPCRs have included the use of membrane-impermeant ligands as negative controls (e.g. [42,48]), there are currently no confirmed membrane-impermeant CB_2 ligands available to test, limiting our ability to delineate surface versus intracellular functional consequences. There are, however, *less* lipophilic CB_2 ligands available that would be interesting to investigate [2,54,55], and the KK318-9EE CB_2 mutant will likely serve as a useful tool in future studies to delineate functions of different CB_2 receptor pools.

The findings of this study indicate that basal CB_2 surface delivery is reliant on a C-terminal KK motif, and ligand-induced anterograde trafficking of CB_2 occurs via an independent pathway that is not downstream of G protein activation, but is likely the result of CB_2 ligands acting as pharmacological chaperones on newly synthesised CB_2. While a range of both agonists and inverse agonists induced this phenotype, it is notable that two specific physiologically/clinically relevant ligands, 2-AG and Δ^9-THC, were unique. The interplay between the effects of endogenous and exogenous ligands on CB_2 subcellular distribution and consequent

signalling from different compartments may have critical impacts on both short- and long-term CB_2-mediated responses. Meanwhile, the potential for CB_2 ligands to interact with intracellular receptors is important to consider in the context of medicinal chemistry efforts where optimisation of physicochemical properties may alter ligand membrane permeability. Further characterisation such as identifying chaperone/adaptor proteins involved may also provide novel therapeutic targets for modulating CB_2 subcellular localisation and, therefore, function.

Statements and Declarations

Funding: This research was funded by a Marsden Fast-Start grant from the Royal Society Te Apārangi New Zealand (UOA1507). CO was supported by a University of Auckland Doctoral Scholarship. NG was supported by Fellowships from the Auckland Medical Research Foundation (1313001) and the Health Research Council of New Zealand (20-006).

Competing Interests: The authors have no relevant financial or non-financial interests to disclose.

Author Contributions: Conceptualisation: NG, MG, CO; Investigation: CO, BW, NG, KW; Methodology: NG, CO; Visualization: CO, KW, NG; Supervision: NG, MG; Funding acquisition: NG; Project administration: NG; Writing – original draft: CO, NG; Writing – review & editing: All authors.

Data Availability: The data that support the findings of this study are available from the corresponding author upon reasonable request.

Ethics approval: Not applicable to this study.

Consent to participate: Not applicable to this study.

Consent to publish: Not applicable to this study.

632 **References**

633 [1] Rakotoarivelo V, Mayer TZ, Simard M, Flamand N, Di Marzo V. The Impact of the CB2 Cannabinoid
634 Receptor in Inflammatory Diseases: An Update. Molecules 2024;29.
635 https://doi.org/10.3390/molecules29143381.

636 [2] Whiting ZM, Yin J, de la Harpe SM, Vernall AJ, Grimsey NL. Developing the Cannabinoid Receptor 2
637 (CB2) pharmacopoeia: past, present, and future. Trends Pharmacol Sci 2022;43:754–71.
638 https://doi.org/10.1016/J.TIPS.2022.06.010.

639 [3] Oyagawa CRM, Grimsey NL. Cannabinoid receptor CB1 and CB2 interacting proteins: Techniques,
640 progress and perspectives. Methods Cell Biol, vol. 166, Academic Press Inc.; 2021, p. 83–132.
641 https://doi.org/10.1016/bs.mcb.2021.06.011.

642 [4] Bouaboula M, Dussossoy D, Casellas P. Regulation of Peripheral Cannabinoid Receptor CB2
643 Phosphorylation by the Inverse Agonist SR 144528: IMPLICATIONS FOR RECEPTOR BIOLOGICAL
644 RESPONSES. Journal of Biological Chemistry 1999;274:20397–405.
645 https://doi.org/10.1074/jbc.274.29.20397.

646 [5] Grimsey NL, Goodfellow CE, Dragunow M, Glass M. Cannabinoid receptor 2 undergoes Rab5-
647 mediated internalization and recycles via a Rab11-dependent pathway. Biochim Biophys Acta
648 2011;1813:1554–60. https://doi.org/10.1016/j.bbamcr.2011.05.010.

649 [6] Kleyer J, Nicolussi S, Taylor P, Simonelli D, Furger E, Anderle P, Gertsch J. Cannabinoid receptor
650 trafficking in peripheral cells is dynamically regulated by a binary biochemical switch. Biochem
651 Pharmacol 2012;83:1393–412. https://doi.org/10.1016/J.BCP.2012.02.014.

652 [7] Chen X, Zheng C, Qian J, Sutton SW, Wang Z, Lv J, Zhou CL and N. Involvement of β-arrestin-2 and
653 Clathrin in Agonist-Mediated Internalization of the Human Cannabinoid CB2 Receptor. Curr Mol
654 Pharmacol 2014;7:67–80. https://doi.org/http://dx.doi.org/10.2174/1874467207666140714115824.

655 [8] Atwood BK, Wager-Miller J, Haskins C, Straiker A, Mackie K. Functional Selectivity in CB(2)
656 Cannabinoid Receptor Signaling and Regulation: Implications for the Therapeutic Potential of CB(2)
657 Ligands. Mol Pharmacol 2012;81:250–63. https://doi.org/10.1124/mol.111.074013.

658 [9] Klauer MJ, Willette BKA, Tsvetanova NG. Functional diversification of cell signaling by GPCR
659 localization. Journal of Biological Chemistry 2024;300. https://doi.org/10.1016/j.jbc.2024.105668.

660 [10] Tóth AD, Turu G, Hunyady L. Functional consequences of spatial, temporal and ligand bias of G
661 protein-coupled receptors. Nature Reviews Nephrology 2024 20:11 2024;20:722–41.
662 https://doi.org/10.1038/s41581-024-00869-3.

663 [11] Brailoiu GC, Deliu E, Marcu J, Hoffman NE, Console-Bram L, Zhao P, Madesh M, Abood ME, Brailoiu
664 E. Differential activation of intracellular versus plasmalemmal CB2 cannabinoid receptors. Biochemistry
665 2014;53:4990–9. https://doi.org/10.1021/bi500632a.

666 [12] Castaneda JT, Harui A, Roth MD. Regulation of Cell Surface CB2 Receptor during Human B Cell
667 Activation and Differentiation. Journal of Neuroimmune Pharmacology 2017;12:544–54.
668 https://doi.org/10.1007/s11481-017-9744-7.

669 [13] Castaneda JT, Harui A, Kiertscher SM, Roth JD, Roth MD. Differential Expression of Intracellular and
670 Extracellular CB2 Cannabinoid Receptor Protein by Human Peripheral Blood Leukocytes. Journal of
671 Neuroimmune Pharmacology 2013;8:323–32. https://doi.org/10.1007/s11481-012-9430-8.

672 [14] Den Boon FS, Chameau P, Schaafsma-Zhao Q, Van Aken W, Bari M, Oddi S, Kruse CG, Maccarrone
673 M, Wadman WJ, Werkmana TR. Excitability of prefrontal cortical pyramidal neurons is modulated by
674 activation of intracellular type-2 cannabinoid receptors. Proc Natl Acad Sci U S A 2012;109:3534–9.
675 https://doi.org/10.1073/PNAS.1118167109.

676 [15] Beerepoot P, Nazari R, Salahpour A. Pharmacological chaperone approaches for rescuing GPCR
677 mutants: Current state, challenges, and screening strategies. Pharmacol Res 2017;117:242–51.
678 https://doi.org/https://doi.org/10.1016/j.phrs.2016.12.036.

[16] Ulloa-Aguirre A, Zariñán T, Gutiérrez-Sagal R, Tao YX. Targeting trafficking as a therapeutic avenue for misfolded GPCRs leading to endocrine diseases. Front Endocrinol (Lausanne) 2022;13:934685. https://doi.org/10.3389/FENDO.2022.934685.

[17] Leidenheimer NJ, Ryder KG. Pharmacological chaperoning: A primer on mechanism and pharmacology. Pharmacol Res 2014;83:10–9. https://doi.org/10.1016/J.PHRS.2014.01.005.

[18] Tao YX, Conn PM. Chaperoning G Protein-Coupled Receptors: From Cell Biology to Therapeutics. Endocr Rev 2014;35:602–47. https://doi.org/10.1210/ER.2013-1121.

[19] Grant MP, Stepanchick A, Cavanaugh A, Breitwieser GE. Agonist-Driven Maturation and Plasma Membrane Insertion of Calcium-Sensing Receptors Dynamically Control Signal Amplitude. Sci Signal 2011;4:ra78 LP-ra78. https://doi.org/10.1126/scisignal.2002208.

[20] Zhao P, Pattison LA, Jensen DD, Jimenez-Vargas NN, Latorre R, Lieu T, Jaramillo JO, Lopez-Lopez C, Poole DP, Vanner SJ, Schmidt BL, Bunnett NW. Protein kinase D and Gβγ mediate sustained nociceptive signaling by biased agonists of protease-activated receptor-2. Journal of Biological Chemistry 2019;294:10649–62. https://doi.org/10.1074/jbc.RA118.006935.

[21] Foyzun T, Whiting M, Velasco KK, Jacobsen JC, Connor M, Grimsey NL. Single nucleotide polymorphisms in the cannabinoid CB2 receptor: Molecular pharmacology and disease associations. Br J Pharmacol 2024;181:2391–412. https://doi.org/10.1111/BPH.16383.

[22] Soethoudt M, Grether U, Fingerle J, Grim TW, Fezza F, de Petrocellis L, Ullmer C, Rothenhäusler B, Perret C, van Gils N, Finlay D, MacDonald C, Chicca A, Gens MD, Stuart J, de Vries H, Mastrangelo N, Xia L, Alachouzos G, Baggelaar MP, Martella A, Mock ED, Deng H, Heitman LH, Connor M, Di Marzo V, Gertsch J, Lichtman AH, Maccarrone M, Pacher P, Glass M, van der Stelt M. Cannabinoid CB(2) receptor ligand profiling reveals biased signalling and off-target activity. Nat Commun 2017;8:13958. https://doi.org/10.1038/ncomms13958.

[23] Cawston EE, Redmond WJ, Breen CM, Grimsey NL, Connor M, Glass M. Real-time characterization of cannabinoid receptor 1 (CB1) allosteric modulators reveals novel mechanism of action. Br J Pharmacol 2013;170:893–907. https://doi.org/10.1111/bph.12329.

[24] Benten WPM, Lieberherr M, Stamm O, Wrehlke C, Guo Z, Wunderlich F. Testosterone Signaling through Internalizable Surface Receptors in Androgen Receptor-free Macrophages. Mol Biol Cell 1999;10:3113–23. https://doi.org/10.1091/mbc.10.10.3113.

[25] von Zastrow M, Kobilka BK. Antagonist-dependent and -independent steps in the mechanism of adrenergic receptor internalization. Journal of Biological Chemistry 1994;269:18448–52. https://doi.org/10.1016/S0021-9258(17)32329-3.

[26] Finlay DB, Joseph WR, Grimsey NL, Glass M. GPR18 undergoes a high degree of constitutive trafficking but is unresponsive to N-Arachidonoyl Glycine. PeerJ 2016;4:e1835. https://doi.org/10.7717/peerj.1835.

[27] Glenn NAK, Finlay DB, Carruthers ER, Mountjoy KG, Walker CS, Grimsey NL. RAMP and MRAP accessory proteins have selective effects on expression and signalling of the CB1, CB2, GPR18 and GPR55 cannabinoid receptors. Br J Pharmacol 2024;181:2212–31. https://doi.org/10.1111/bph.16095.

[28] Grimsey NL, Narayan PJ, Dragunow M, Glass M. A Novel High-Throughput Assay for the Quantitative Assessment of Receptor Trafficking. Clin Exp Pharmacol Physiol 2008;35:1377–82. https://doi.org/10.1111/j.1440-1681.2008.04991.x.

[29] Grimsey NL, Graham ES, Dragunow M, Glass M. Cannabinoid Receptor 1 trafficking and the role of the intracellular pool: Implications for therapeutics. Biochem Pharmacol 2010;80:1050–62. https://doi.org/10.1016/j.bcp.2010.06.007.

[30] Shaffer JP. Modified Sequentially Rejective Multiple Test Procedures. J Am Stat Assoc 1986;81:826–31. https://doi.org/10.2307/2289016.

[31] Chan WY, Soloviev MM, Ciruela F, McIlhinney RAJ. Molecular Determinants of Metabotropic Glutamate Receptor 1B Trafficking. Molecular and Cellular Neuroscience 2001;17:577–88. https://doi.org/https://doi.org/10.1006/mcne.2001.0965.

[32] Upadhyaya J, Singh N, Bhullar RP, Chelikani P. The structure–function role of C-terminus in human bitter taste receptor T2R4 signaling. Biochimica et Biophysica Acta (BBA) - Biomembranes 2015;1848:1502–8. https://doi.org/https://doi.org/10.1016/j.bbamem.2015.03.035.

[33] Zhang X, Dong C, Wu QJ, Balch WE, Wu G. Di-acidic Motifs in the Membrane-distal C Termini Modulate the Transport of Angiotensin II Receptors from the Endoplasmic Reticulum to the Cell Surface. Journal of Biological Chemistry 2011;286:20525–35. https://doi.org/10.1074/jbc.M111.222034.

[34] Zhang X, Wang H, Duvernay MT, Zhu S, Wu G. The angiotensin II type 1 receptor C-terminal Lys residues interact with tubulin and modulate receptor export trafficking. PLoS One 2013;8:e57805–e57805. https://doi.org/10.1371/journal.pone.0057805.

[35] Kay EI, Botha R, Montgomery JM, Mountjoy KG. hMRAPa specifically alters hMC4R molecular mass and N-linked complex glycosylation in HEK293 cells. J Mol Endocrinol 2013;50:217–27. https://doi.org/10.1530/JME-12-0220.

[36] Samson M-T, Small-Howard A, Shimoda LMN, Koblan-Huberson M, Stokes AJ, Turner H. Differential Roles of CB1 and CB2 Cannabinoid Receptors in Mast Cells. The Journal of Immunology 2003;170:4953–62. https://doi.org/10.4049/jimmunol.170.10.4953.

[37] Filppula S, Yaddanapudi S, Mercier R, Xu W, Pavlopoulos S, Makriyannis A. Purification and mass spectroscopic analysis of human CB2 cannabinoid receptor expressed in the baculovirus system. The Journal of Peptide Research 2004;64:225–36. https://doi.org/10.1111/j.1399-3011.2004.00188.x.

[38] Klausner RD, Donaldson JG, Lippincott-Schwartz J. Brefeldin A: insights into the control of membrane traffic and organelle structure. J Cell Biol 1992;116:1071–80. https://doi.org/10.1083/jcb.116.5.1071.

[39] Mollenhauer HH, Morré DJ, Rowe LD. Alteration of intracellular traffic by monensin; mechanism, specificity and relationship to toxicity. Biochim Biophys Acta 1990;1031:225–46. https://doi.org/10.1016/0304-4157(90)90008-z.

[40] Schneider-Poetsch T, Ju J, Eyler DE, Dang Y, Bhat S, Merrick WC, Green R, Shen B, Liu JO. Inhibition of eukaryotic translation elongation by cycloheximide and lactimidomycin. Nat Chem Biol 2010;6:209–17. https://doi.org/10.1038/nchembio.304.

[41] Mouillac B, Mendre C. Vasopressin receptors and pharmacological chaperones: From functional rescue to promising therapeutic strategies. Pharmacol Res 2014;83:74–8. https://doi.org/https://doi.org/10.1016/j.phrs.2013.10.007.

[42] Petäjä-Repo UE, Hogue M, Bhalla S, Laperrière A, Morello J-P, Bouvier M. Ligands act as pharmacological chaperones and increase the efficiency of delta opioid receptor maturation. EMBO J 2002;21:1628–37. https://doi.org/10.1093/emboj/21.7.1628.

[43] Chaipatikul V, Erickson-Herbrandson LJ, Loh HH, Law P-Y. Rescuing the Traffic-Deficient Mutants of Rat μ-Opioid Receptors with Hydrophobic Ligands. Mol Pharmacol 2003;64:32 LP – 41. https://doi.org/10.1124/mol.64.1.32.

[44] Chen Y, Chen C, Wang Y, Liu-Chen L-Y. Ligands Regulate Cell Surface Level of the Human κ Opioid Receptor by Activation-Induced Down-Regulation and Pharmacological Chaperone-Mediated Enhancement: Differential Effects of Nonpeptide and Peptide Agonists. Journal of Pharmacology and Experimental Therapeutics 2006;319:765 LP – 775. https://doi.org/10.1124/jpet.106.107987.

[45] Shim SM, Choi HR, Sung KW, Lee YJ, Kim ST, Kim D, Mun SR, Hwang J, Cha-Molstad H, Ciechanover A, Kim BY, Kwon YT. The endoplasmic reticulum-residing chaperone BiP is short-lived and metabolized through N-terminal arginylation. Sci Signal 2018;11. https://doi.org/10.1126/scisignal.aan0630.

[46] Dallavilla T, Abrami L, Sandoz PA, Savoglidis G, Hatzimanikatis V, van der Goot FG. Model-Driven Understanding of Palmitoylation Dynamics: Regulated Acylation of the Endoplasmic Reticulum Chaperone Calnexin. PLoS Comput Biol 2016;12:e1004774. https://doi.org/10.1371/journal.pcbi.1004774.

[47] Carruthers ER, Grimsey NL. Cannabinoid CB2 receptor orthologues; in vitro function and perspectives for preclinical to clinical translation. Br J Pharmacol 2024;181:2247–69. https://doi.org/10.1111/BPH.16172.

[48] Morello JP, Salahpour A, Laperrière A, Bernier V, Arthus MF, Lonergan M, Petäjä-Repo U, Angers S, Morin D, Bichet DG, Bouvier M. Pharmacological chaperones rescue cell-surface expression and function of misfolded V2 vasopressin receptor mutants. Journal of Clinical Investigation 2000;105:887–95. https://doi.org/10.1172/JCI8688.

[49] Ibsen MS, Finlay DB, Patel M, Javitch JA, Glass M, Grimsey NL. Cannabinoid CB1 and CB2 Receptor-Mediated Arrestin Translocation: Species, Subtype, and Agonist-Dependence. Front Pharmacol 2019;10:350. https://doi.org/10.3389/fphar.2019.00350.

[50] Patel M, Grimsey NL, Banister SD, Finlay DB, Glass M. Evaluating signaling bias for synthetic cannabinoid receptor agonists at the cannabinoid CB2 receptor. Pharmacol Res Perspect 2023;11:e01157. https://doi.org/10.1002/PRP2.1157.

[51] Ashton JC. The use of knockout mice to test the specificity of antibodies for cannabinoid receptors. Hippocampus 2012;22:643–4. https://doi.org/10.1002/hipo.20946.

[52] Marchalant Y, Brownjohn PW, Bonnet A, Kleffmann T, Ashton JC. Validating Antibodies to the Cannabinoid CB2 Receptor: Antibody Sensitivity Is Not Evidence of Antibody Specificity. Journal of Histochemistry & Cytochemistry 2014;62:395–404. https://doi.org/10.1369/0022155414530995.

[53] Li Y, Kim J. Neuronal expression of CB2 cannabinoid receptor mRNAs in the mouse hippocampus. Neuroscience 2015;311:253–67. https://doi.org/https://doi.org/10.1016/j.neuroscience.2015.10.041.

[54] Oyagawa CRM, de la Harpe SM, Saroz Y, Glass M, Vernall AJ, Grimsey NL. Cannabinoid Receptor 2 Signalling Bias Elicited by 2,4,6-Trisubstituted 1,3,5-Triazines. Front Pharmacol 2018;9:1202. https://doi.org/10.3389/fphar.2018.01202.

[55] Sharma R, Singh S, Whiting ZM, Molitor M, Vernall AJ, Grimsey NL. Novel Cannabinoid Receptor 2 (CB2) Low Lipophilicity Agonists Produce Distinct cAMP and Arrestin Signalling Kinetics without Bias. Int J Mol Sci 2023;24:6406. https://doi.org/10.3390/IJMS24076406/S1.

Fig. 1

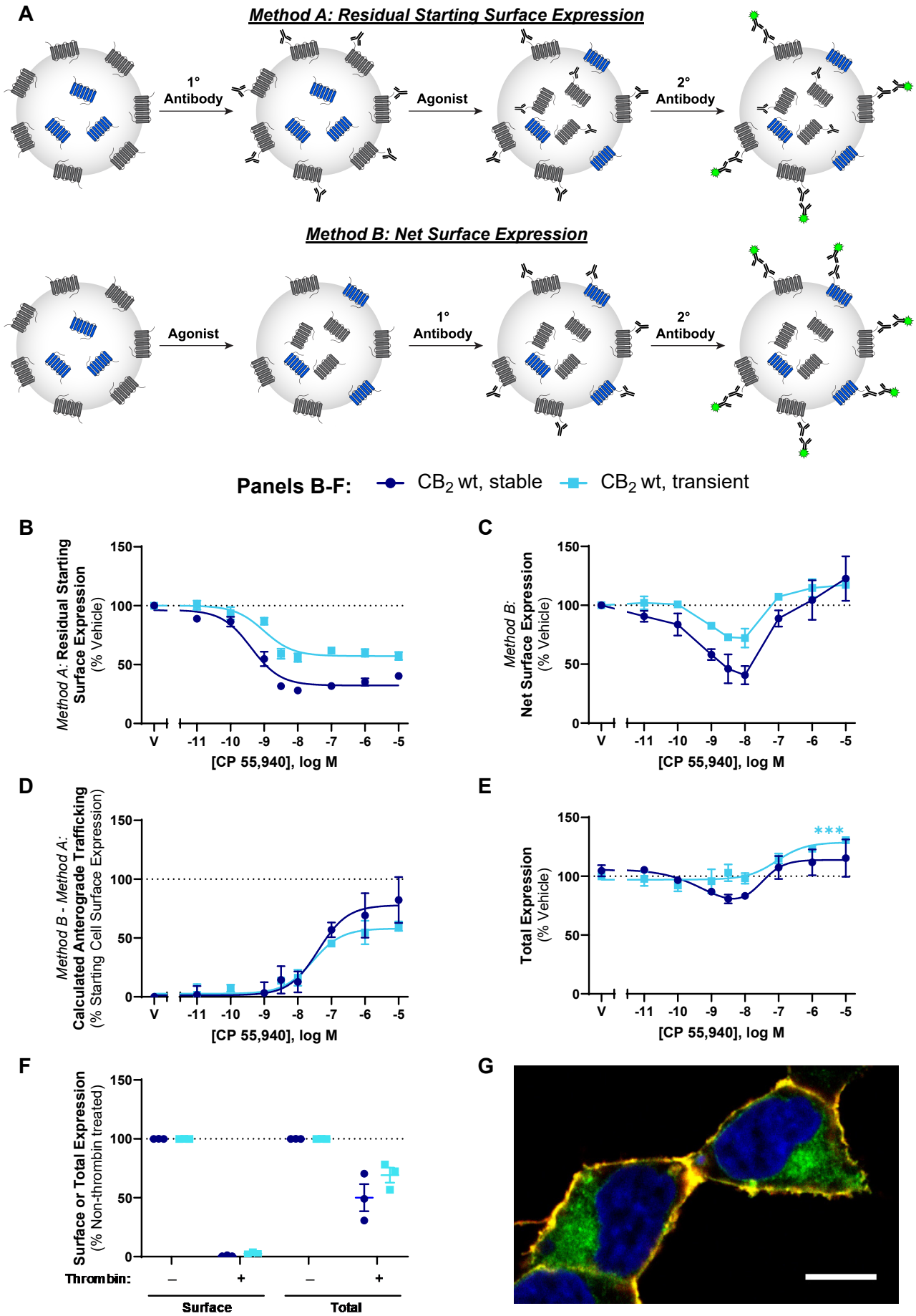
A
Method A: Residual Starting Surface Expression
1° Antibody
Agonist
2° Antibody
Method B: Net Surface Expression
Agonist
1° Antibody
2° Antibody
Panels B-F:
CB2 wt, stable
CB2 wt, transient
B
Method A: Residual Starting Surface Expression (% Vehicle)
[CP 55,940], log M
C
Method B: Net Surface Expression (% Vehicle)
[CP 55,940], log M
D
Method B - Method A: Calculated Anterograde Trafficking (% Starting Cell Surface Expression)
[CP 55,940], log M
E
Total Expression (% Vehicle)
***
[CP 55,940], log M
F
Surface or Total Expression (% Non-thrombin treated)
Thrombin:
Surface
Total
G

Fig. 1 CB_2 trafficking in response to CP 55,940

(A) Immunocytochemical approaches used to measure surface receptor expression. *Method A* - cells are labelled with primary antibody directed against an extracellular epitope tag on the receptor of interest, followed by stimulation with agonist. Cells are then incubated with secondary antibody under non-permeabilising conditions, to label residual primary antibody at the cell surface. *Method B* - cells are stimulated with agonist, then labelled with primary antibody to an extracellular epitope tag under non-permeabilising conditions. This labels receptors present at the cell surface at the end of drug stimulation. Cells are then fixed and secondary antibody applied. (B, C, E) HEK cells stably or transiently expressing hCB_2 wt were treated with a CP 55,940 dilution series for 3 hours, and were labelled to measure (B) residual starting surface expression (*Method A*), (C) net surface expression (*Method B*), or (E) total receptor expression (i.e. primary antibody applied under permeabilising conditions to detect both cell surface and intracellular receptor). (D) Calculated anterograde trafficking (*Method B* – *Method A*). (F) Surface and total CB_2 expression without and with exposure to thrombin (to cleave surface HA epitopes) prior to fixation. (B-F) Data are presented as mean ± SEM from three independent experiments. (G) Confocal image illustrating surface (red/yellow) and intracellular (green) CB_2. Nuclei are stained blue. Scale bar, 10μm.

Fig. 2

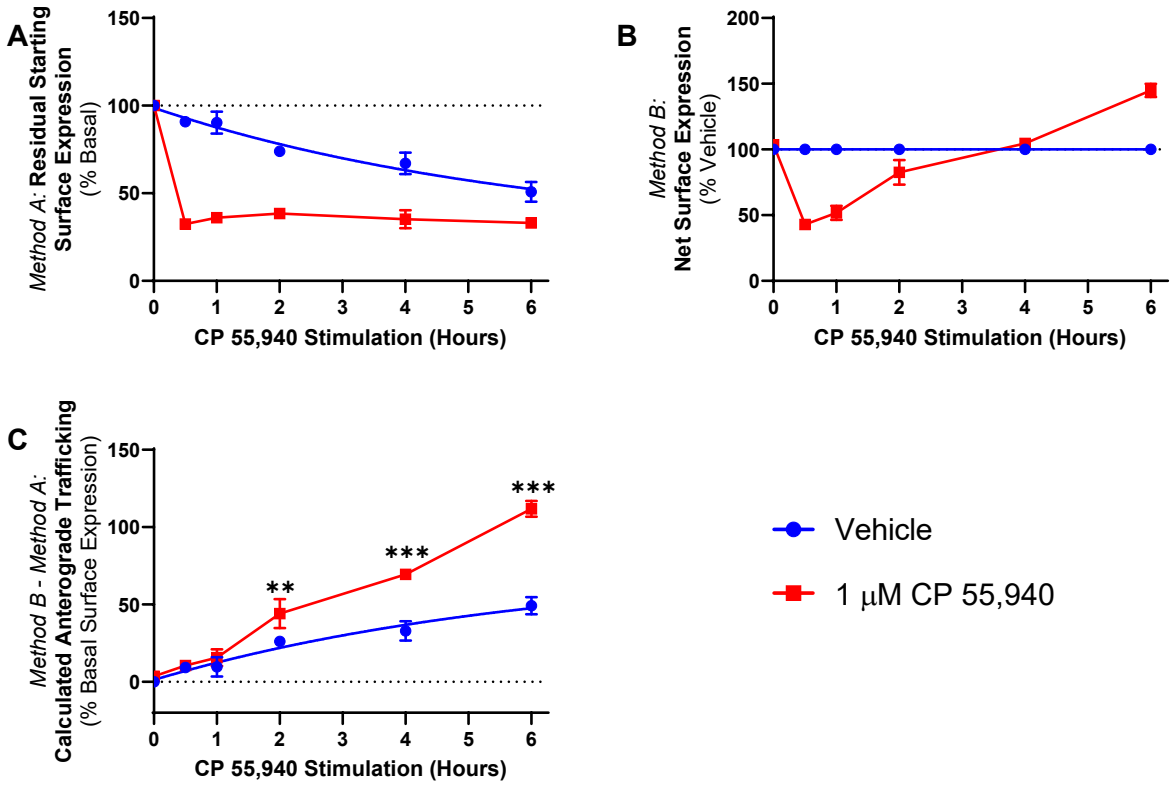

Fig. 2 CB_2 trafficking time course in response to CP 55,940

HEK cells stably expressing CB_2 wt were treated with 1 μM CP 55,940 or vehicle over a 6 h time course, and labelled to measure (A) residual starting surface expression (*Method A*) or (B) net surface expression (*Method B*). (C) Calculated anterograde trafficking (*Method B – Method A*). *P* values for significant differences between Vehicle and CP 55,940 are indicated graphically as: ** < 0.005, *** < 0.001. Data are presented as mean ± SEM from three independent experiments.

Fig. 3

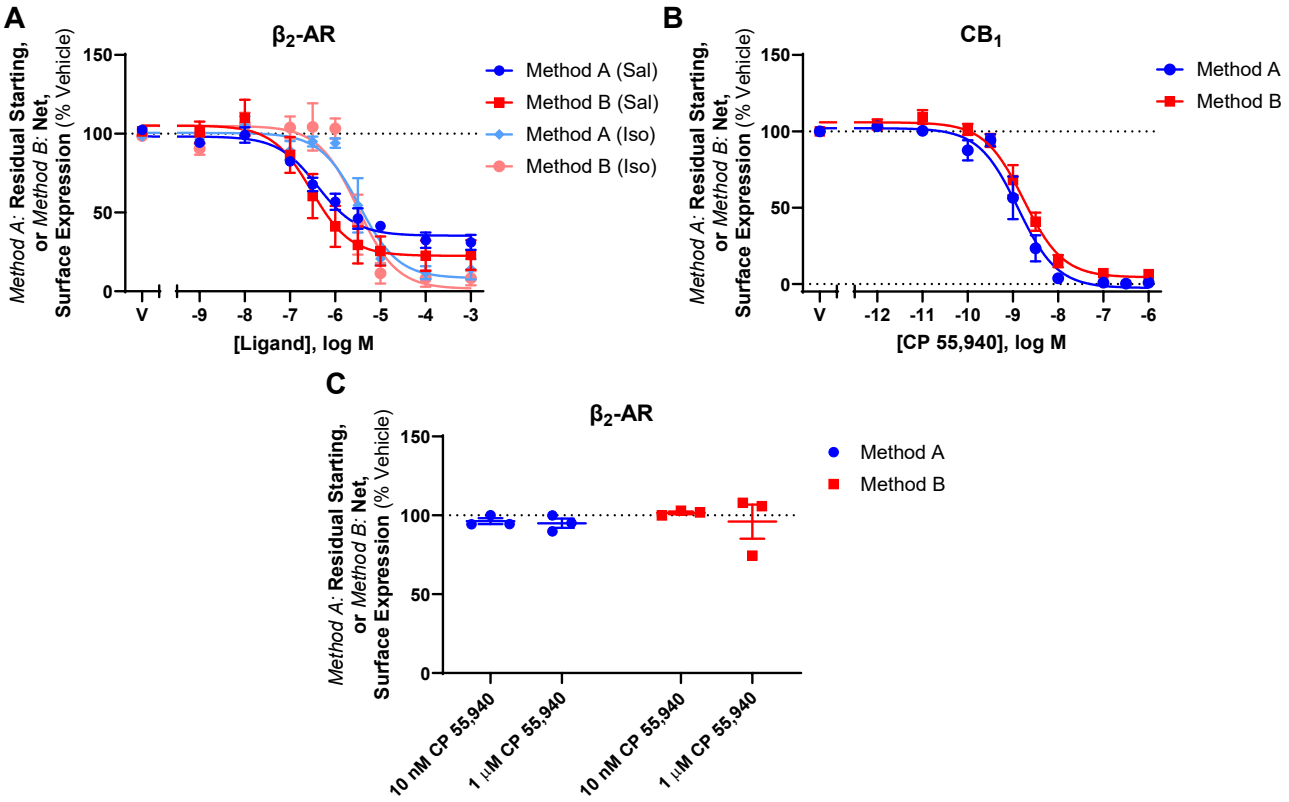

Fig. 3 Trafficking of β_2-AR and CB_1

HEK cells stably expressing β_2-AR were treated with (A) a Salbutamol (Sal) or Isoproterenol (Iso) dilution series, or (C) an internalising (10 nM) or anterograde trafficking-inducing (1 μM) concentration of CP 55,940 for 3 h. (B) HEK cells stably expressing CB_1 were treated with a CP 55,940 dilution series for 3 h. Residual starting surface expression (*Method A*) and net surface expression (*Method B*) were measured in all assays. Data are presented as mean ± SEM from three independent experiments.

Fig. 4

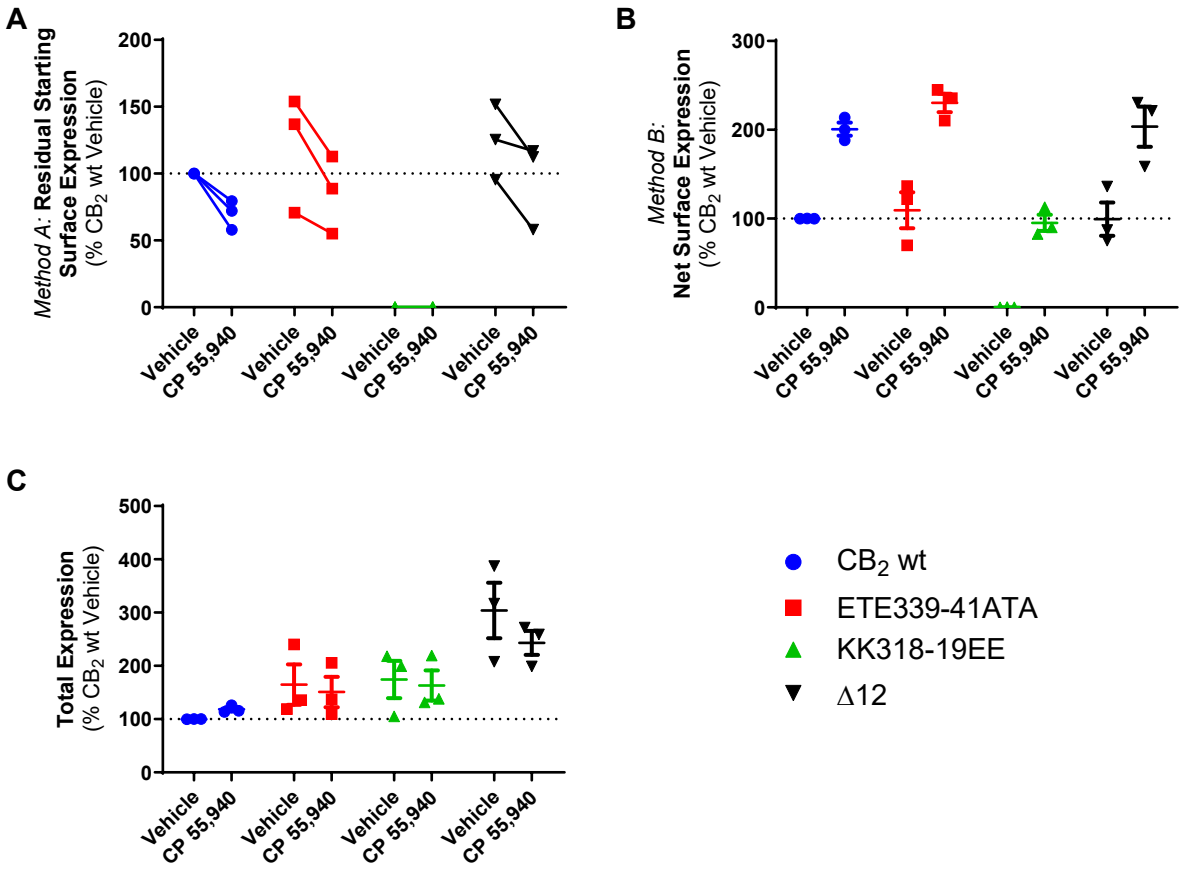

Fig. 4 Trafficking of CB_2 mutant constructs in response to CP 55,940

HEK cells transiently expressing CB_2 wt or CB_2 mutants were treated with vehicle or 1 μM CP 55,940 for 3 h and labelled to measure (A) residual starting surface expression (*Method A*), (B) net surface expression (*Method B*), or (C) total receptor expression. Data are presented as mean ± SEM from three independent experiments, except in Panel A where matched data from each of three independent experiments is plotted.

Fig. 5

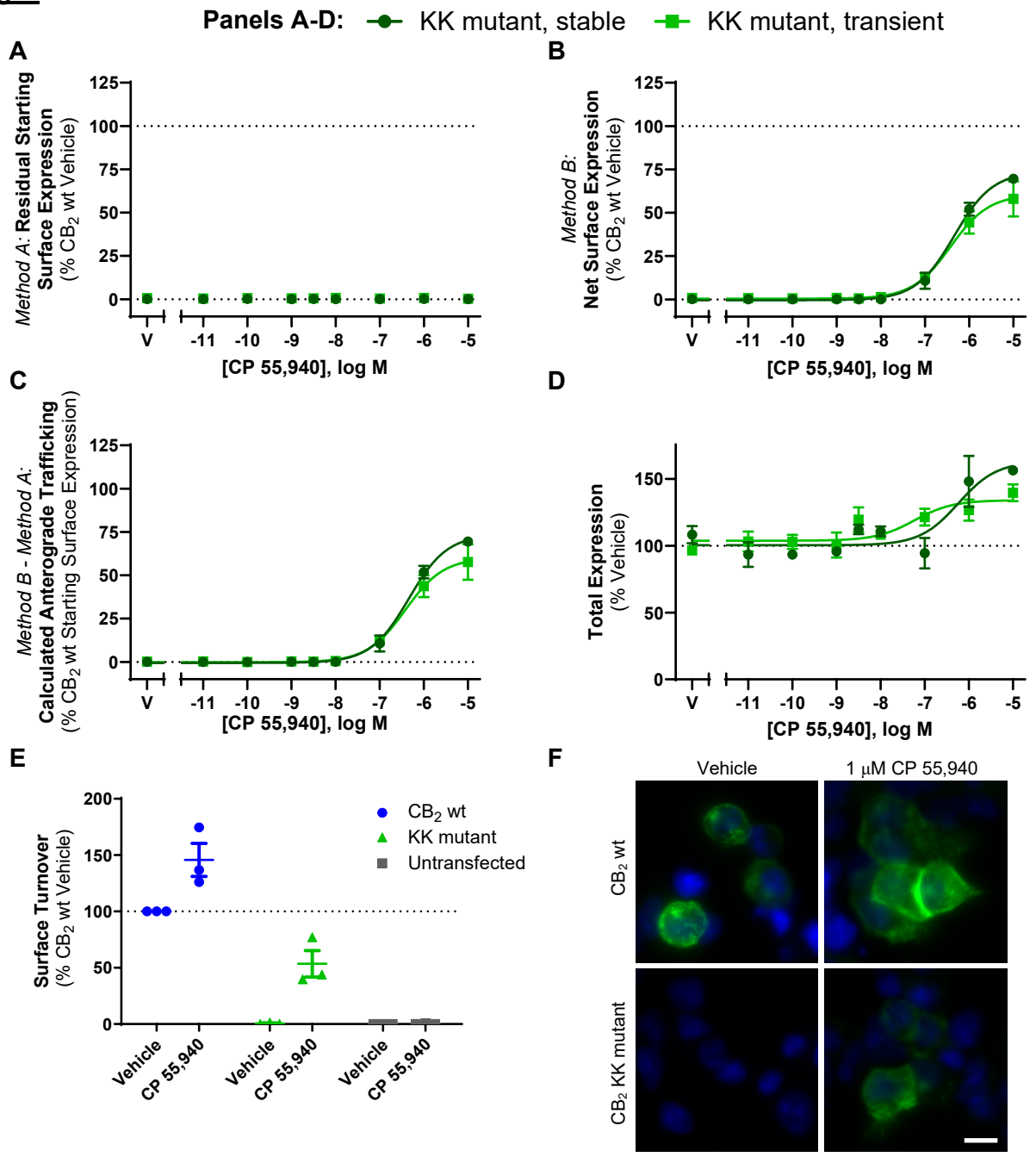

Fig. 5 CB_2 KK mutant trafficking and expression in response to CP 55,940

HEK cells stably and transiently expressing KK mutant were treated with a CP 55,940 dilution series for 3 h and were labelled to measure (A) residual starting surface expression (*Method A*), (B) net surface expression (*Method B*), or (D) total receptor expression. (C) Calculated anterograde trafficking (*Method B – Method A*). Data are presented as mean ± SEM from three independent experiments. (E-F) HEK cells transiently expressing CB_2 wt or KK mutant were treated with vehicle or 1 μM CP 55,940 for 3 h in the continued presence of primary anti-HA to measure surface turnover. (E) Mean ± SEM from three independent experiments. (F) Scale bar = 10 μM. Representative of three independent experiments.

Fig. 6

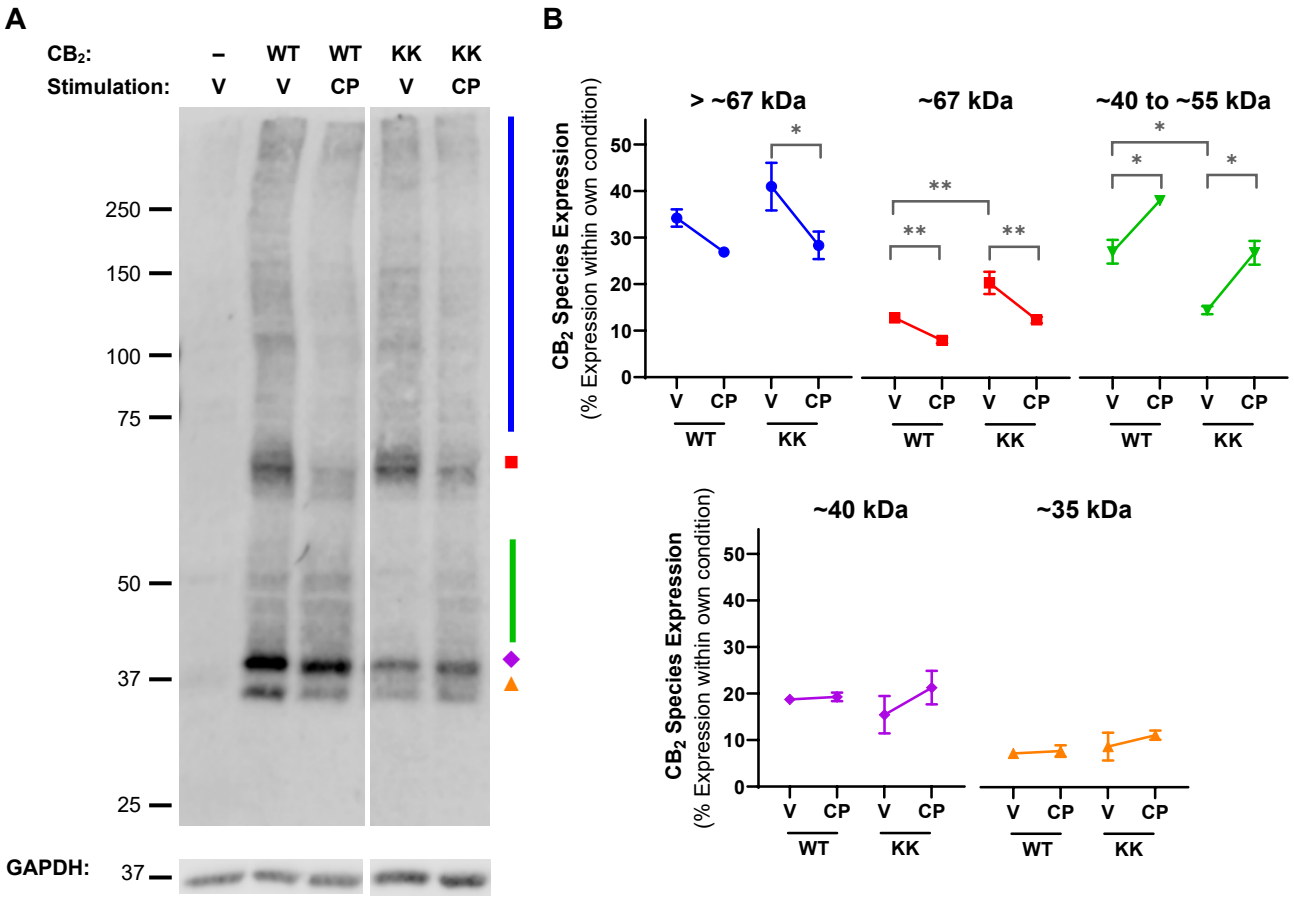

Fig. 6 Western blot analysis for CB_2 wt and KK mutant

HEK Flp-in cells transiently expressing CB_2 wt ("WT"), KK mutant ("KK"), or benign vector, were treated with vehicle (V) or 1 μM CP 55,940 (CP) for 3 hours. (A) Western blot for anti-HA to detect CB_2 (top panel) or GAPDH control protein (bottom panel). Molecular weight markers shown in kDa. All lanes are from the same membrane and displayed at the same intensity, but re-arranged for presentation. Representative of three independent experiments. (B) Each distinct band, or molecular weight range, was normalised to the total signal from the entire lane within the same experimental condition – i.e. each is represented as a percentage of total receptor expression. *P* values for significant differences between Vehicle and CP 55,940 or WT and KK (comparisons indicated by brackets) are indicated graphically as: * <0.05, ** < 0.005. Data are presented as mean ± SEM of three independent experiments.

Fig. 7

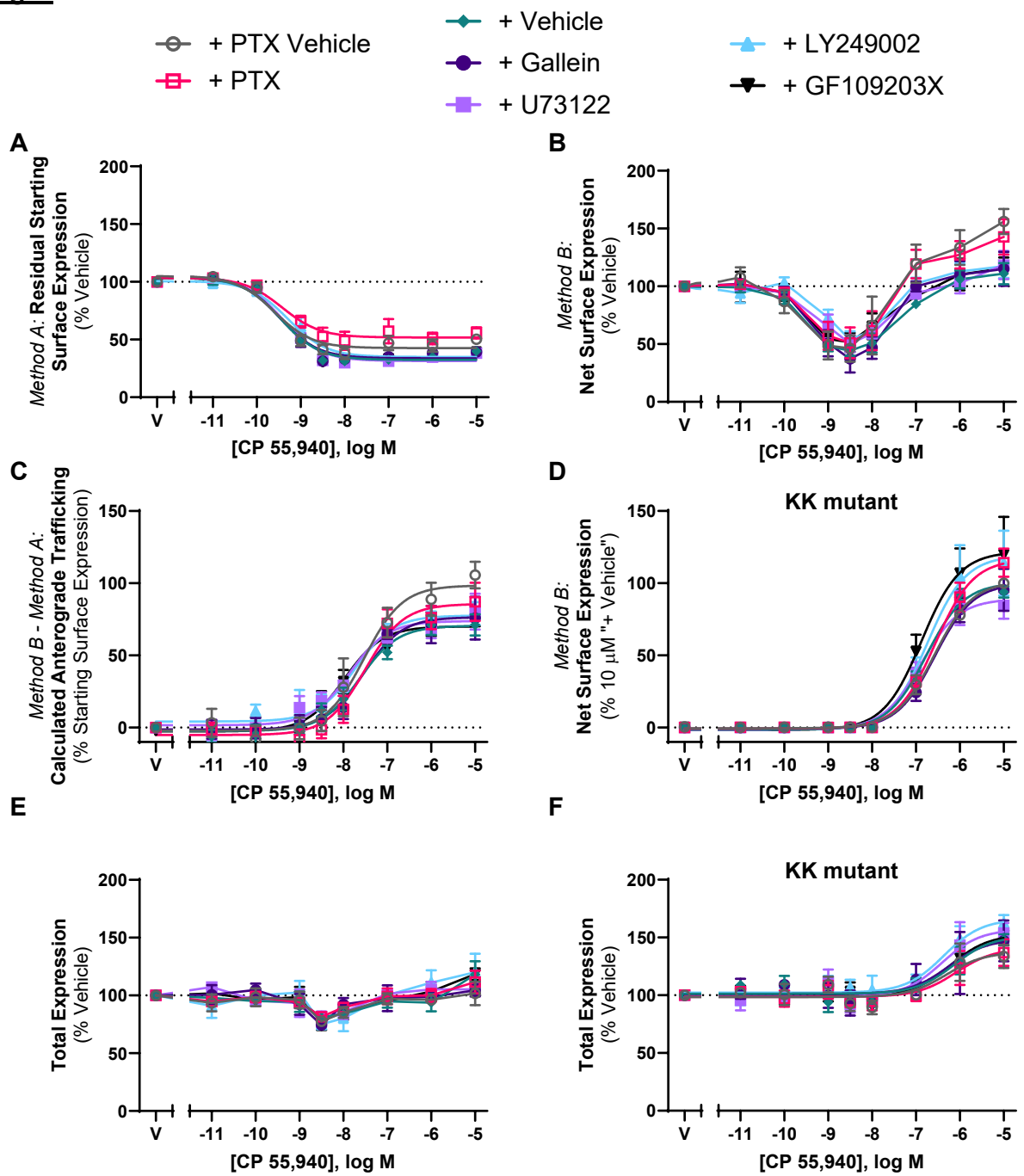

Fig. 7 CB_2 wt and KK mutant trafficking in response to CP 55,940 in the presence of various signalling inhibitors

HEK cells stably expressing CB_2 wt (A, B, C, E) or KK mutant (D, F) were treated with a CP 55,940 dilution series for 3 h, in the absence or presence of various signalling inhibitors, and were labelled to measure (A) residual starting surface expression (*Method A*), (B, D) net surface expression (*Method B*), or (E, F) total receptor expression. (C) Calculated CB_2 wt anterograde trafficking (*Method B – Method A*). Data are presented as mean ± SEM from three independent experiments (except inhibitor vehicle in A-D, n=6).

Fig. 8

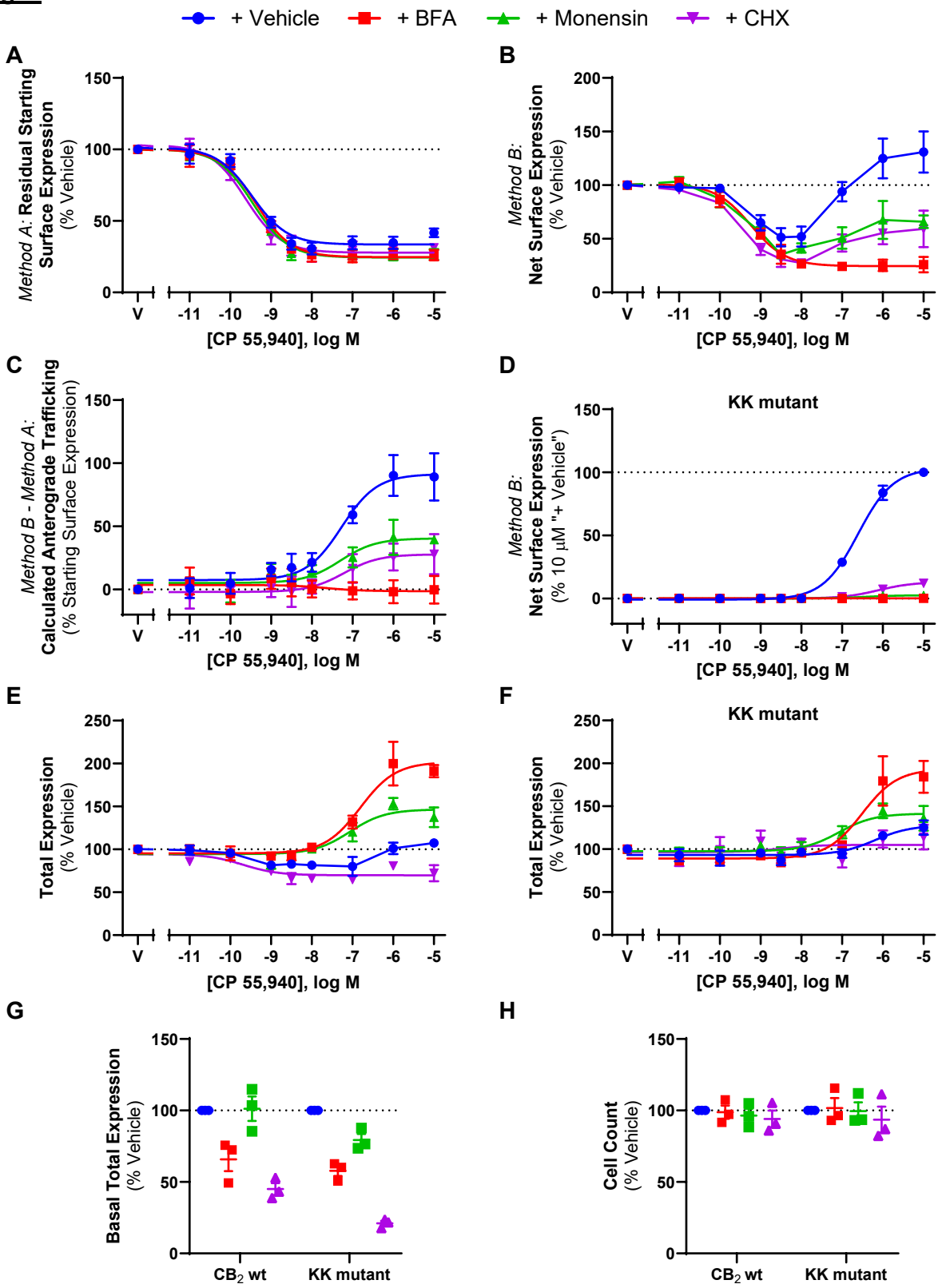

Fig. 8 CB_2 wt and KK mutant trafficking in response to CP 55,940 in the presence of various trafficking-related inhibitors

HEK Flp-in cells stably expressing CB_2 wt (A, B, C, E) or KK mutant (D & F) were treated with a CP 55,940 dilution series for 3 hours, in the absence or presence of trafficking or protein synthesis inhibitors, and were labelled to measure (A) residual starting surface expression (*Method A*), (B, D) net surface expression (*Method B*), or (E, F) total receptor expression. (C) Calculated CB_2 wt anterograde trafficking (*Method B* – *Method A*). (G) Basal total expression, and (H) average cell count from 'G'. Data are presented as mean ± SEM from three independent experiments.

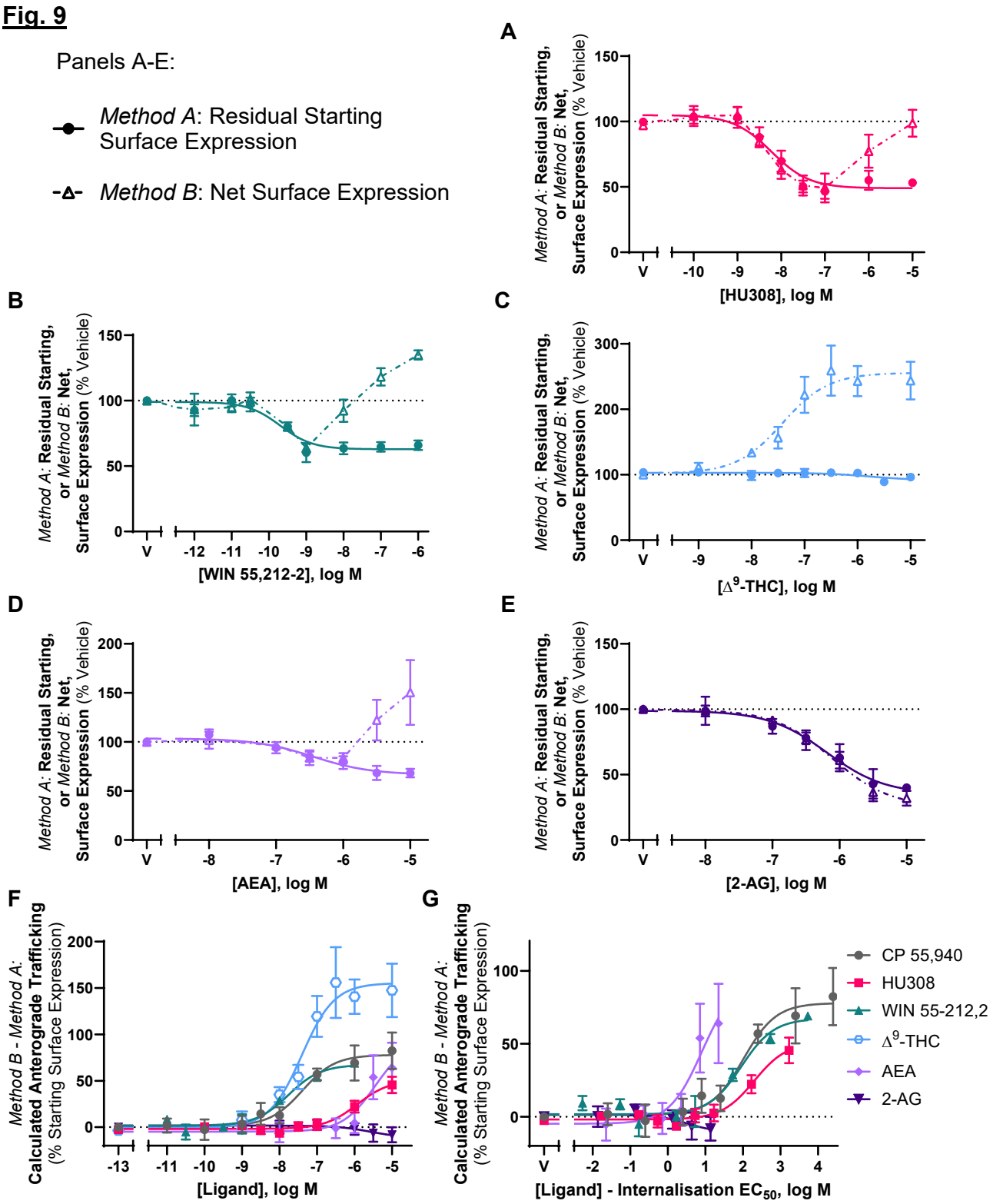

Fig. 9 CB_2 wt trafficking in response to a panel of CB_2 agonists

Cells stably expressing CB_2 wt were treated with dilution series of various CB_2 agonists for 3 hours and labelled to measure (A-E) residual starting surface expression (*Method A*) or net surface expression (*Method B*). (F) Calculated ligand-induced CB_2 wt anterograde trafficking (*Method B – Method A* from panels A-E; CP 55,940 re-plotted from Fig. 1D). (G) Calculated ligand-induced

anterograde trafficking from panel F, normalised on the x-axis to each ligand's respective internalisation $EC_{50,}$ wherein the internalisation $logEC_{50}$ was subtracted from the treatment concentrations. Data are presented as mean ± SEM from three independent experiments (except AEA, n=4).

Fig. 10

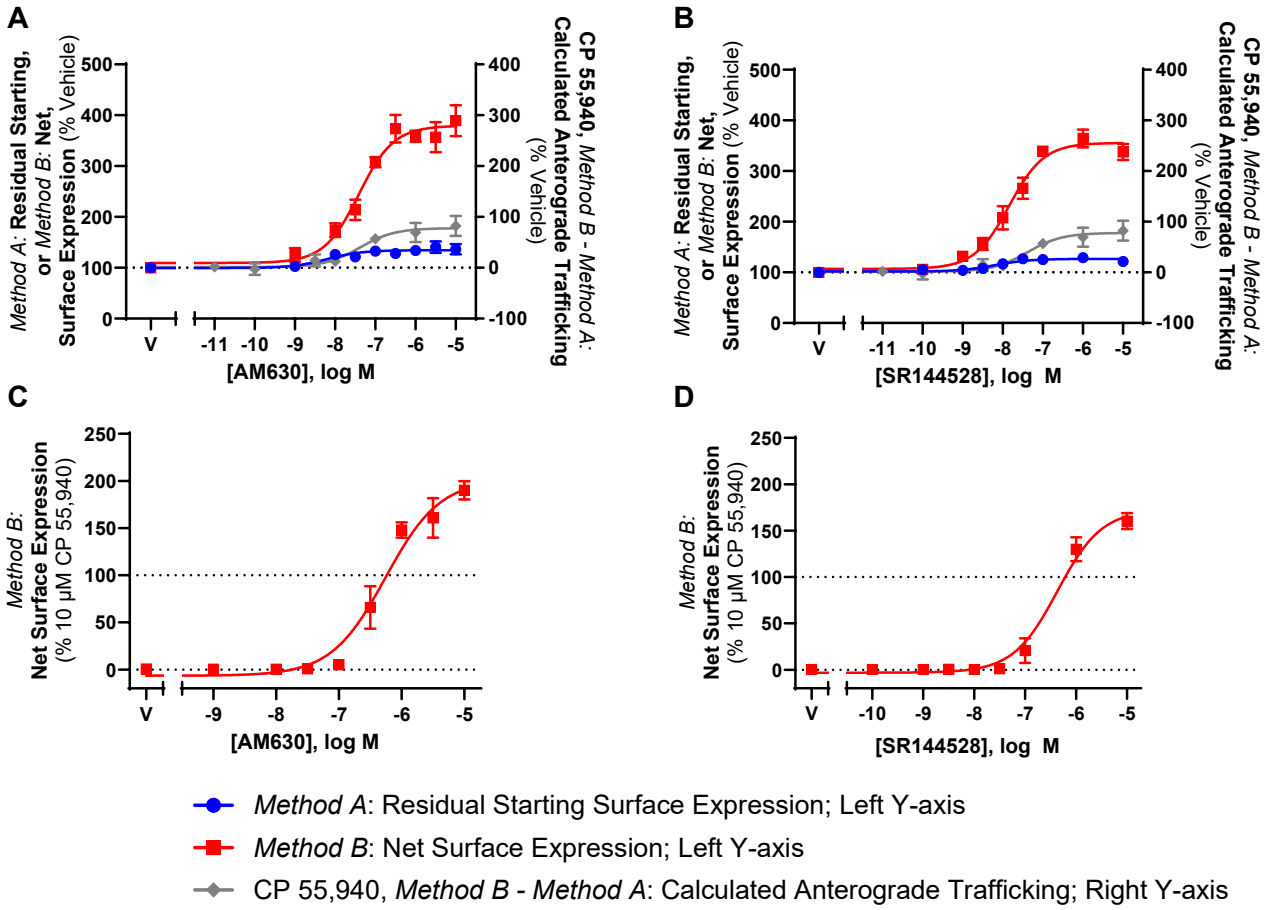

Fig. 10. CB_2 wt and KK mutant trafficking in response to CB_2 inverse agonists

Left Y-axis: Cells stably expressing (A,B) CB_2 wt or (C,D) KK mutant were treated with dilution series of CB_2-selective inverse agonists, AM630 and SR 144528, for 3 hours, and were labelled to measure residual starting surface expression (*Method A*) or net surface expression (*Method B*). Right Y-axis: In A-B, calculated CP 55,940-induced anterograde trafficking (*Method B – Method B*) is shown for reference. Data are presented as mean ± SEM from three independent experiments.

Table 1. Summary data for stably- and transiently-expressed CB_2 trafficking in response to CP 55,940. Parameters are derived from data shown in Fig. 1B and 1D, from three independent experiments.

	Method A: **Internalisation (3 hour)**		*Method B – Method A:* **Calculated Anterograde Trafficking (3 hour)**	
	pEC_{50} (± SEM)	**E_{max}, % Vehicle** (± SEM)	**pEC_{50}** (± SEM)	**E_{max}, % Starting Surface Expression, Vehicle** (± SEM)
Stable CB_2 wt	9.40 (0.09)	-64.4 (2.4)	7.35 (0.17)	76.6 (10.0)
Transient CB_2 wt	9.09 (0.19)	-43.4 (2.4)	7.66 (0.29)	56.7 (5.5)

Table 2. Summary data for stably- and transiently-expressed CB_2 KK mutant trafficking in response to CP 55,940. Parameters are derived from data shown in Fig. 5C, from three independent experiments.

	Method B – Method A: **Calculated Anterograde Trafficking (3 hour)**	
	pEC_{50} (± SEM)	**E_{max}, % CB_2 wt Vehicle** (± SEM)
Stable CB_2 KK mutant	6.35 (0.11)	74.3 (2.7)
Transient CB_2 KK mutant	6.42 (0.11)	60.86 (10.2)

Table 3. Trafficking summary data for stably expressed CB_2 and KK mutant in response to CP 55,940, in the absence or presence of various inhibitors of signalling, trafficking, or protein synthesis. Parameters are derived from three independent experiments, unless otherwise stated.

	Method A: **Internalisation (3 hour)**		*Method B – Method A:* **CP 55,940-Induced Anterograde Trafficking (3 hour)**			
	CB_2 wt		**CB_2 wt**		**KK mutant**	
	pEC_{50} (± SEM)	**E_{max}, % Vehicle** (± SEM)	**pEC_{50}** (± SEM)	**E_{max}, % Starting Surface Expression, Vehicle** (± SEM)	**pEC_{50}** (± SEM)	**E_{max}#** (± SEM)
+ PTX Vehicle	9.60 (0.05)	-62.7 (4.9)	7.56 (0.24)	102.4 (8.6)	6.59 (0.12)	102.1 (2.4)
+ PTX ($G\alpha_{i/o}$ & $G\beta\gamma$ inhibitor)	9.40 (0.02)	-52.3 (9.4)	7.42 (0.07)	90.1 (7.4)	6.59 (0.08)	117.3 (12.5)
+ Vehicle*	9.46 (0.05)	-71.6 (1.7)	7.64 (0.13)	73.8 (8.1)	6.75 (0.10)	102.9 (2.2)
+ Gallein ($G\beta\gamma$ inhibitor)	9.47 (0.05)	-71.1(2.8)	7.58 (0.14)	78.4 (13.0)	6.57 (0.09)	101.2 (13.9)
+ U73122 (PLC inhibitor)	9.42 (0.02)	-72.5 (1.8)	7.83 (0.12)	72.6 (7.3)	6.87 (0.10)	90.8 (10.8)
+ LY249002 (PI3K inhibitor)	9.43 (0.02)	-66.7 (1.5)	7.74 (0.14)	73.1 (4.0)	6.72 (0.03)	120.5 (23.7)
+ GF109203X (PKC inhibitor)	9.45 (0.05)	-71.1 (2.2)	7.96 (0.15)	73.2 (1.8)	6.87 (0.13)	124.3 (23.8)
+ Vehicle^	9.48 (0.04)	-67.9 (3.9)	7.30 (0.18)	71.6 (14.3)	6.60 (0.04)	104.3 (2.1)
+ BFA	9.38 (0.04)	-75.5 (3.1)	-	-	-	-
+ Monensin	9.45 (0.02)	-75.7 (4.2)	7.35 (0.18)	36.4 (8.0)	-	2.7 (1.0)
+ CHX	9.56 (0.06)	-74.1 (1.1)	7.20 (0.12)	29.3 (11.4)	6.18 (0.15)	13.1 (3.0)

KK mutant CP 55,940-induced anterograde trafficking E_{max} is normalised to the efficacy measured at 10 μM for the "+ Vehicle" conditions. *All parameters derived from 6 independent experiments. ^All parameters derived from 4 independent experiments.

Table 4. Trafficking summary data for stably expressed CB_2 and KK mutant in response to various CB_2 ligands. Parameters are derived from three independent experiments, unless otherwise stated.

	Method A: **Internalisation (3 hour)**		*Method B – Method A:* **Calculated Anterograde Trafficking (3 hour)**			*Method B:* **Net Surface Expression (3 hour)**	
	CB_2 wt		**CB_2 wt**			**KK mutant**	
	pEC_{50} (± SEM)	**E_{max}** (± SEM)[a]	**pEC_{50}** (± SEM)	**Internalisation-Adjusted EC_{50}** (± SEM)[b]	**E_{max}** (± SEM)[c]	**pEC_{50}** (± SEM)	**E_{max}** (± SEM)[d]
CP 55,940°	9.40 (0.09)	-64.4 (2.4)	7.35 (0.17)	2.05 (0.25)	+76.6 (10.0)	N.D.[+]	N.D.[+]
HU308	8.23 (0.10)	-56.3 (3.1)	5.91 (0.19)	2.32 (0.29)	+53.7 (7.0)	N.D.	N.D.
WIN 55,212-2	9.73 (0.12)	-37.3 (1.6)*	7.76 (0.16)	1.97 (0.08)	+65.7 (4.6)	N.D.	N.D.
Δ^9-THC	Not measurable	-3.7 (3.6)^	7.43 (0.16)	Not measurable	+158.5 (32.5)**	N.D.	N.D.
AEA	6.35 (0.16)	-42.1 (6.0)*	Not measurable	Not measurable	+63.9 (27.1)[#]	N.D.	N.D.
2-AG	6.13 (0.20)	-67.6 (4.1)	Not measurable	Not measurable	-8.2 (8.2)^	N.D.	N.D.
AM630	8.17 (0.14)	+35.1 (6.0)	7.36 (0.06)	0.81 (0.18)	+238.9 (10.8)	6.29 (0.12)	209.3 (20.6)
SR144528	8.15 (0.19)	+25.9 (1.2)	7.82 (0.20)	0.33 (0.39)	+229.5 (2.8)	6.37 (0.15)	178.4 (10.7)

N.D. = Not determined. [a]Internalisation E_{max} represented as reduction (−) or increase (+) in surface expression, as a percentage of vehicle-treated control. [b]Internalisation-adjusted anterograde trafficking EC_{50} calculated for each ligand by subtracting the EC_{50} for internalisation from the anterograde trafficking EC_{50}. [c]Anterograde trafficking was calculated by subtracting internalisation (*Method A*, normalised to vehicle-treated control) from net surface expression (*Method B*, normalised to vehicle-treated control). E_{max} is therefore represented as reduction (−) or increase (+), as a percentage of starting surface expression. [d]KK mutant net surface expression Emax is normalised to that induced by 10 μM CP 55,940 at the same timepoint. °CP 55,940 data for CB2 wt is re-tabulated from Table 1 (adding new calculation for internalisation-adjusted EC_{50}). [#]A fully defined concentration-response curve could not be obtained, therefore efficacy at the highest concentration tested (i.e., 10 μM) is noted instead of E_{max}. ^A concentration-response curve could not be fitted, therefore efficacy at the highest concentration tested (i.e., 10 μM) is noted instead of $E_{max.}$ [+]Not determined in this experiment set. See Table 2 for data. *$p < 0.05$ vs. CP 55,940 and 2-AG. **$p < 0.05$ vs. HU308, WIN 55,212-2, 2-AG and AEA.